THE JOURNAL OF BIOLOGICAL CHEMISTRY
Vol. 276, No. 36, Issue of September 7, pp. 33596–33607, 2001
Printed in U.S.A.

Protein Kinase A-mediated Phosphorylation of Serine 357 of the Mouse Prostacyclin Receptor Regulates Its Coupling to G_s-, to G_i-, and to G_q-coupled Effector Signaling*

Received for publication, May 16, 2001, and in revised form, June 28, 2001
Published, JBC Papers in Press, July 6, 2001, DOI 10.1074/jbc.M104434200

Orlaith A. Lawler, Sinead M. Miggin, and B. Therese Kinsella‡

From the Department of Biochemistry, Conway Institute of Biomolecular and Biomedical Research, Merville House, University College Dublin, Belfield, Dublin 4, Ireland

The prostacyclin receptor (IP) is primarily coupled to $G\alpha_s$-dependent activation of adenylyl cyclase; however, a number of studies indicate that the IP may couple to other secondary effector systems perhaps in a species-specific manner. In the current study, we investigated the specificity of G protein:effector coupling by the mouse (m) IP overexpressed in human embryonic kidney 293 cells and endogenously expressed in murine erythroleukemia cells. The mIP exhibited efficient $G\alpha_s$ coupling and concentration-dependent increases in cAMP generation in response to the IP agonist cicaprost; however, mIP also coupled to $G\alpha_i$ decreasing the levels of cAMP in forskolin-treated cells. mIP coupling to $G\alpha_i$ was pertussis toxin-sensitive and was dependent on protein kinase (PK) A activation status. In addition, the mIP coupled to phospholipase C (PLC) activation in a pertussis toxin-insensitive, $G\alpha_i$-, $G\beta\gamma$-, and PKC-independent but in a $G\alpha_q$- and PKA-dependent manner. Whole cell phosphorylation assays demonstrated that the mIP undergoes cicaprost-induced PKA phosphorylation. mIP^{S357A}, a site-directed mutant of mIP, efficiently coupled to $G\alpha_s$ but failed to couple to $G\alpha_i$ or to efficiently couple to $G\alpha_q$:PLC. Moreover, mIP^{S357A} did not undergo cicaprost-induced phosphorylation confirming that Ser^{357} is the target residue for PKA-dependent phosphorylation. Finally, co-precipitation experiments permitted the detection of $G\alpha_s$, $G\alpha_i$, and $G\alpha_q$ in the immunoprecipitates of mIP, whereas only $G\alpha_s$ was co-precipitated with mIP^{S357A} indicating that Ser^{357} of mIP is essential for $G\alpha_i$ and $G\alpha_q$ interaction. Moreover, inhibition of PKA blocked co-precipitation of mIP with $G\alpha_i$ or $G\alpha_q$. Taken together our data indicate that the mIP, in addition to coupling to $G\alpha_s$, couples to $G\alpha_i$ and $G\alpha_q$; however, $G\alpha_i$ and $G\alpha_q$ coupling is dependent on initial cicaprost-induced mIP:$G\alpha_s$ coupling and phosphorylation of mIP by cAMP-dependent PKA where Ser^{357} was identified as the target residue for PKA phosphorylation.

The prostanoid prostacyclin (prostaglandin I_2), mainly produced by the vascular endothelium, plays a key role in the local control of vascular hemostasis acting as a potent inhibitor of platelet aggregation and as a vasodilator (1, 2). The actions of prostacyclin generally counteract those of thromboxane A_2, and thus, the relative levels of these two prostanoids in the circulation are central to the maintenance of vascular hemostasis and vessel tone (3). Prostacyclin also exhibits proinflammatory and antiproliferative properties *in vitro* (4, 5) and may confer a cytoprotective effect against tissue injury during acute myocardial ischemia or in response to hypoxia (6).

Prostacyclin signals through interaction with its signature G protein-coupled receptor (GPCR)[1] termed IP (7). The prostacyclin receptor (IP) is primarily coupled to activation of adenylyl cyclase via G_s (3, 8, 9). Additional evidence indicates that the IP may couple to multiple G protein:effector systems including G_q-dependent activation of PLC and to mobilization of intracellular calcium (10–13). Iloprost, a stable carbacyclin analogue of prostacyclin, can stimulate the opening of ATP-sensitive K^+ channels resulting in hyperpolarization and relaxation of the canine carotid artery (14). The IP agonists iloprost and cicaprost were shown to stimulate the GTPase activity of both G_s and G_i suggesting that the IP expressed in human erythroleukemia cells may potentially lead to activation and inhibition of adenylyl cyclase, respectively (15). On the other hand, the IP expressed in the rat medullary thick ascending limb coupled exclusively to G_i inhibiting adenylyl cyclase as opposed to G_s (16).

We have recently established that the IP may be unique among GPCRs in that it is isoprenylated (12). Whereas isoprenylation of mouse (m) IP is not required for ligand binding, it is absolutely required for its activation of adenylyl cyclase and for its efficient coupling to PLC (12, 13). In addition, a number of studies have confirmed that the IP undergoes rapid agonist-induced receptor phosphorylation, internalization/sequestration, and down-regulation in human platelets and other cell types (10, 17–20).

Whereas the primary manifestation of GPCR phosphorylation and sequestration was classically thought to be desensitization or dampening of the signal following agonist engagement, there is increasing evidence that this is not exclusively so (21). In fact, it is now widely held, for certain GPCRs at least, that "desensitization of the primary signaling event" may trig-

* This research was supported by grants (to B. T. K) from The Irish Heart Foundation, Enterprise Ireland, The Wellcome Trust, and The Health Research Board of Ireland. The costs of publication of this article were defrayed in part by the payment of page charges. This article must therefore be hereby marked "*advertisement*" in accordance with 18 U.S.C. Section 1734 solely to indicate this fact.

‡ To whom correspondence should be addressed: Dept. of Biochemistry, Merville House, University College Dublin, Belfield, Dublin 4, Ireland. Tel.: 353-1-7161507; Fax: 353-1-2837211; E-mail: Therese.Kinsella@UCD.IE.

[1] The abbreviations used are: GPCR, G protein-coupled receptor; β_2AR, β_2-adrenergic receptor; βARK1, β-adrenergic receptor kinase 1; HA, hemagglutinin; HEK, human embryonic kidney; IP, prostacyclin receptor; IP_3, inositol 1,4,5-trisphosphate; MEL, murine erythroleukemia; PK, protein kinase; PLC, phospholipase C; MES, 4-morpholineethanesulfonic acid; HBS, HEPES-buffered saline; PI-PLC, phosphatidylinositol-specific phospholipase C; PAGE, polyacrylamide gel electrophoresis; PVDF, polyvinylidene difluoride; C-tail, carboxyl-terminal tail.

ger the "activation of (an)other secondary signaling cascade(s)" (21). For example, for many GPCRs, receptor phosphorylation and subsequent internalization has been shown to be essential for GPCR activation of the mitogen-activated protein kinase cascades and for transactivation of growth factor receptors (22). Moreover, in a limited number of cases, agonist-mediated receptor phosphorylation has been reported to trigger *molecular switching* whereby a receptor alters its coupling from one G protein:effector system to a different G protein:effector system (23, 24). Such molecular switching can facilitate GPCR coupling to more than one G protein:effector system (21).

The molecular mechanisms whereby a single IP can couple to more than one G protein:effector system has not been explored in detail. Thus, in the present study we investigated the G protein coupling characteristics of the mIP stably overexpressed in human embryonic kidney (HEK) 293 cells and in murine erythroleukemia (MEL) cells, which endogenously express mIP. Our studies confirmed that mIP, in addition to its coupling to $G\alpha_s$, may also couple $G\alpha_i$ and $G\alpha_q$ through a mechanism involving initial $G\alpha_s$ signaling and cAMP-dependent protein kinase (PK) A phosphorylation of mIP at Ser^{357} within its C-tail region; thereafter the phosphorylated mIP exhibited coupling to pertussis toxin (PTx)-sensitive $G\alpha_i$ and inhibition of adenylyl cyclase and to $G\alpha_q$-mediated activation of PLC. These studies provide essential evidence demonstrating that agonist activation of the classical G_s-coupled mIP can trigger its phosphorylation and, in turn, favor its signaling to G_i- and G_q-coupled signal transduction cascades.

EXPERIMENTAL PROCEDURES

Materials

Cicaprost was obtained from Schering AG (Berlin, Germany). Iloprost, [^{3}H]iloprost (15.3 Ci/mmol), and [^{3}H]CGP-12177 (41.0 Ci/mmol) were purchased from Amersham Pharmacia Biotech. Fura2/AM, D-*myo*-inositol 1,4,5-trisphosphate, and its 3-deoxyhexasodium salt (stable analogue of IP_3) were purchased from Calbiochem. [^{32}P]Orthophosphate (8,000–9,000 Ci/mmol) was obtained from PerkinElmer Life Sciences. Isoproterenol was purchased from Sigma. [^{3}H]IP_3 (20–40 Ci/mmol) and [^{3}H]cAMP (15–30 Ci/mmol) were purchased from American Radiolabeled Chemicals Inc. Polyvinylidene difluoride (PVDF) filters, *Taq* DNA polymerase, the chemiluminescence Western blotting kit, and rat monoclonal 3F10 anti-hemagglutinin (HA) peroxidase-conjugated antibody were purchased from Roche Molecular Biochemicals. Oligonucleotides were synthesized by Genosys Biotechnologies. Anti-$G\alpha_s$ (K-20), $G\alpha_{q/11}$ (C-19), and $G\alpha_{i\text{-}1}$ (I-20) antisera, horseradish peroxidase-conjugated goat anti-rabbit IgG, and anti-G protein-coupled receptor kinase 2 (C-15) antibody, raised against the carboxyl terminus of the β-adrenergic receptor kinase 1, were obtained from Santa Cruz Biotechnology. Mouse monoclonal 101R anti-HA antibody was obtained from BabCO.

Materials and Methods

Site-directed Mutagenesis of the mIP—Conversion of Ser^{357} of the mIP to Ala^{357}, herein designated mIP^{S357A}, was performed using the Stratagene Quick Change site-directed mutagenesis kit using pHM:mIP (12) as template and oligonucleotides 5′-CTT TCC AGA CCT GCA ***GCG*** GGG AGA AGA GAC C-3′ (sense primer) and 5′-G GTC TCT TCT CCC ***CGC*** TGC AGG TCT GGA AAG-3′ (antisense primer, the sequence complimentary to mutator Ser (TCG) to Ala (GCG) codon is in boldface italics). The plasmid was verified by double-stranded DNA sequencing using Sequenase Version 2.0 (United States Biochemical Corp.). The plasmid pRK5·βARK1-(495–689) encoding the carboxyl-terminal amino acid residues 495–689 of βARK1 (25) was kindly provided by Prof. Robert Lefkowitz, Howard Hughes Medical Institute, Duke University Medical Center. The plasmid pCMV·$G\alpha_i$ was generated by subcloning the full-length cDNA for rat $G\alpha_{i\text{-}1}$ into the *Eco*RI site of pCMV5. The plasmids pCMV·$G\alpha_q$ and pCMV·$G\alpha_s$ have been described previously (12, 26).

Cell Culture and Transfections—MEL clone 707 cells and HEK 293 cells were obtained from the American Type Culture Collection and were maintained at 37 °C in 5% CO_2. MEL cells were routinely cultured in Dulbecco's modified Eagle's medium, 20% fetal bovine serum. HEK 293 cells were cultured in minimal essential medium with Earle's salts and 10% fetal bovine serum.

HEK 293 cells were transfected with 10 μg of pADVA and 25 μg of pCMV- or pHM-based vectors using the calcium phosphate/DNA coprecipitation procedure (26). For transient transfections, cells were harvested 48 h after transfection. HEK.mIP, HEK.HAmIP, HEK.mIP^{SSLC}, and HEK.β_2AR cell lines have been previously described (12). To create the HEK.$HAmIP^{S357A}$ stable cell line, HEK 293 cells were transfected with 10 μg of *Sca*I-linearized pADVA plus 25 μg of *Pvu*I-linearized pHM:mIP^{S357A}. Forty-eight hours post-transfection, G418 (0.8 mg/ml) selection was applied. After ~21 days, G418-resistant colonies were selected, and individual HEK.$HAmIP^{S357A}$ pure clonal stable cell lines or isolates were examined for IP expression by radioligand binding. All isolates used throughout the study were derived from pure clonal stable cell lines.

Radioligand Binding Studies—Cells were harvested by centrifugation at 500 × *g* at 4 °C for 5 min and washed three times with phosphate-buffered saline. For membrane preparation, cells were resuspended in Homogenization Buffer (25 mM Tris-HCl, pH 7.5, 0.25 M sucrose, 10 mM $MgCl_2$, 1 mM EDTA, 0.1 mM phenylmethylsulfonyl fluoride), and membrane fractions were prepared by homogenization followed by centrifugation (100,000 × *g*, 40 min at 4 °C). The pellet fraction (P_{100}), representing crude membranes, was resuspended in Resuspension Buffer (10 mM MES-KOH, pH 6.0, 10 mM $MnCl_2$, 1 mM EDTA, 10 mM indomethacin). IP radioligand binding assays were carried out at 30 °C for 1 h using 100 μg of membrane protein (P_{100}) in 100-μl reactions in the presence of 4 nM [^{3}H]iloprost (15.3 Ci/mmol) as described previously (12). β_2-Adrenergic receptor (β_2AR) radioligand binding assays were carried out on whole cells using 25 nM [^{3}H]CGP-12177 (41.0 Ci/mmol) at 14 °C for 3 h using 100 μg of protein in a final volume of 100 μl essentially as described previously (27). Protein determinations were carried out using the Bradford assay (28).

Measurement of cAMP—cAMP assays were carried out as described previously (12). Briefly, cells were harvested by scraping and were washed three times in ice-cold phosphate-buffered saline. Cells (~1–2 × 10^6 cells) were resuspended in 200 μl of HEPES-buffered saline (HBS; 140 mM NaCl, 4.7 mM KCl, 2.2 mM $CaCl_2$, 1.2 mM KH_2PO_4, 11 mM glucose, 15 mM HEPES-NaOH, pH 7.4) containing 1 mM 3-isobutyl-1-methylxanthine and were preincubated at 37 °C for 10 min. Thereafter ligands (50 μl) were added, and cells were stimulated at 37 °C for 10 min in the presence of the ligand (1 μM cicaprost, 10 μM forskolin, 1 μM cicaprost plus 10 μM forskolin, 10 μM isoproterenol, or 10 μM isoproterenol plus 10 μM forskolin). For concentration-response studies, cells were stimulated with 1 pM–1 μM cicaprost. As controls, cells were incubated in the presence of 50 μl of HBS in the absence of ligand. To investigate the effect of PTx, cells were preincubated with PTx (50 ng/ml) for 16 h prior to stimulation with the respective ligand. To investigate the effect of kinase inhibitors on cAMP generation, cells were preincubated in the presence of GF 109203X (50 nM), H-89 (10 μM), or vehicle (HBS) at 37 °C for 10 min prior to stimulation with the respective ligand. In separate experiments, to examine the effect of co-transfection of $G\alpha_s$ on cAMP generation, HEK 293, HEK.mIP, and HEK.mIP^{S357A} cells were transiently co-transfected with pCMV·$G\alpha_s$ (25 μg/10-cm dish) plus pADVA (10 μg/10-cm dish).

In each case, cAMP reactions were terminated by heat inactivation at 100 °C for 5 min, and the level of cAMP produced was quantified using the cAMP-binding protein assay (12). Levels of cAMP produced by ligand-treated cells over basal stimulation, determined in the presence of HBS, were expressed as pmol of cAMP/mg of cell protein ± S.E. Results are expressed as -fold stimulation relative to basal (-fold increase ± S.E.). Data were analyzed using the unpaired Student's *t* test. *p* values of less than or equal to 0.05 were considered to indicate a statistically significant difference.

Measurement of IP_3 Levels—Intracellular IP_3 levels were measured as described previously (29, 30). Briefly, cells were harvested, washed twice in ice-cold phosphate-buffered saline and were then resuspended at ~5 × 10^6 cells/ml in HBS containing 10 mM LiCl. To investigate the effect of PTx, cells were preincubated with PTx (50 ng/ml) for 16 h prior to harvesting. To investigate the effect of the kinase inhibitors, H-89 (10 μM) or GF 109203X (50 nM) was added, and the cells were incubated for 5 min at 37 °C in 5% CO_2 prior to harvesting. Cells (200 μl) were then preincubated at 37 °C for 10 min. Thereafter cells were stimulated for 2 min at 37 °C in the presence of cicaprost (1 μM), or for concentration-response studies, cells were stimulated with 1 nM–10 μM cicaprost. To determine basal IP_3 levels, cells were incubated in the presence of an equivalent volume (50 μl) of the vehicle HBS. To examine the effect of co-transfection of $G\alpha_q$ on IP_3 generation, HEK.mIP cells were transiently co-transfected with pCMV·$G\alpha_q$ (12) (25 μg/10-cm dish) and

pADVA (10 μg/10-cm dish). The IP_3 levels produced were determined using the IP_3-binding protein assay (29, 30). Levels of IP_3 produced by ligand-stimulated cells over basal stimulation in the presence of HBS were expressed in pmol of IP_3/mg of cell protein ± S.E., and results are presented as -fold stimulation over basal (-fold increase ± S.E.). The data presented are representative of four independent experiments, each performed in duplicate.

Measurement of Intracellular [Ca^{2+}] Mobilization—Measurements of $[Ca^{2+}]_i$ in Fura2/AM-preloaded cells were carried out essentially as described previously (26). To investigate the effect of PTx, cells were preincubated with PTx (50 ng/ml) at 37 °C in 5% CO_2 for 16 h prior to stimulation with cicaprost (1 μM). Where appropriate, the PKA (H-89, 10 μM) or PKC (GF 109203X, 50 nM) kinase inhibitors were added 2 min prior to stimulation with cicaprost (1 μM). The phosphatidylinositol-specific phospholipase C (PI-PLC) (U73122, 1 μM) and phosphatidylcholine-specific phospholipase C (D-609, 10 μM) inhibitors were added 5 min prior to stimulation of cells with cicaprost (1 μM). Drugs and inhibitors, with stock solutions dissolved in ethanol or dimethyl sulfoxide, were diluted in HBSSHB (modified Ca^{2+}/Mg^{2+}-free Hanks' buffered salt solution containing 20 mM HEPES, pH 7.67, 0.1% bovine serum albumin plus 1 mM $CaCl_2$) to the appropriate concentration such that the addition of 20 μl of the diluted drug/inhibitor to 2 ml of cells resulted in the correct working concentration. In separate experiments to examine the effect of Gβγ on $[Ca^{2+}]_i$ mobilization, HEK.mIP cells were transiently co-transfected with the plasmid pRK5·βARK1-(495–689) encoding amino acid residues 459–689 from the C-tail of βARK1 (25 μg/10-cm dish) plus pADVA (10 μg/10-cm dish). For each $[Ca^{2+}]_i$ measurement, calibration of the fluorescence signal was performed in 0.2% Triton X-100 to obtain the maximal fluorescence (R_{max}) and 1 mM EGTA to obtain the minimal fluorescence (R_{min}). The ratio of the fluorescence at 340 and 380 nm is a measure of $[Ca^{2+}]_i$ assuming a K_d of 225 nM Ca^{2+} for Fura2/AM. The results presented in the figures are representative data from at least four independent experiments and were plotted as changes (Δ) in $[Ca^{2+}]_i$ mobilized as a function of time (s) upon ligand stimulation or, alternatively, were calculated as mean changes in $[Ca^{2+}]_i$ mobilized (Δ$[Ca^{2+}]_i$ ± S.E.; $n = 4$).

Western Blot Analysis—HEK.HAmIP or HEK.HAmIP^{S357A} cells were transfected with 10 μg of pADVA and 25 μg of pRK5·βARK1-(459–689) or 25 μg of pCMV·Gα_s, pCMV·Gα_i, or pCMV·Gα_q using the calcium phosphate/DNA co-precipitation procedure (26). Cells were harvested 48 h post-transfection, and aliquots of whole cell protein (75 μg) were resuspended in 1× Solubilization Buffer (10% β-mercaptoethanol (v/v), 2% SDS (w/v), 30% glycerol (v/v), 0.025% bromphenol blue (w/v), 50 mM Tris-HCl, pH 6.8; 100 μl) and boiled for 5 min. Samples were then resolved by SDS-polyacrylamide gel electrophoresis (PAGE) and were electroblotted onto PVDF membranes (12). Thereafter membranes were screened by immunoblot analysis using either the anti-G protein-coupled receptor kinase 2 (C-15; 1:2000) antibody, directed against the carboxyl terminus of βARK1, or the appropriate anti-Gα_s (K-20) (1:3000), G$\alpha_{q/11}$ (C-19) (1:3000), or G$\alpha_{i\text{-}1}$ (I-20) (1:500) antisera. Horseradish peroxidase-conjugated goat anti-rabbit IgG (1:3000) was used as the secondary antibody in each case. Proteins were visualized using the chemiluminescence detection system according to the manufacturer's recommendations.

Measurement of Agonist-mediated IP Phosphorylation in Whole Cells—Agonist-mediated IP phosphorylations in whole HEK.HAmIP (isolate 2 cells) and HEK.HAmIP^{S357A} cells were carried out essentially as described previously (29). Briefly, cells were washed once in phosphate-free Dulbecco's modified Eagle's medium containing 10% dialyzed fetal bovine serum and were metabolically labeled for 1 h in the same media (1.5 ml/10-cm dish) containing 100 μCi/ml [^{32}P]orthophosphate (8,000–9,000 Ci/mmol) at 37 °C in 5% CO_2. Where appropriate, H-89 (10 μM), GF 109203X (50 nM), or the vehicle HBS was added for the duration of the labeling period. Thereafter 1 μM cicaprost or the vehicle HBS was added for 10 min at 37 °C in 5% CO_2. Metabolic labeling of cells was terminated by transferring the dishes to ice and aspiration of the medium. Thereafter cells were quickly washed once in ice-cold phosphate-buffered saline (2 ml/dish) and were lysed with 0.6 ml of Radioimmune Precipitation Buffer (50 mM Tris-HCl, pH 8.0, 150 mM NaCl, 1 mM EDTA, 1% Nonidet P-40 (v/v), 0.5% sodium deoxycholate (w/v), 0.1% SDS (w/v) containing 10 mM sodium fluoride, 25 mM sodium pyrophosphate, 10 mM ATP, 1 μg/ml leupeptin, 10 μg/ml soybean trypsin inhibitor, 1 mM benzamidine hydrochloride, 0.5 mM phenylmethylsulfonyl fluoride, 1 mM sodium orthovanadate). Following a 15-min incubation on ice, cells were harvested and disrupted by sequentially passing through hypodermic needles of decreasing bore size (G20, G21, G23, and G26), and soluble cell lysates were harvested by centrifugation for 15 min at 13,000 × *g* at room temperature. HA epitope-tagged IP receptors were immunoprecipitated using the anti-HA antibody (101R, 1:300 dilution) at room temperature for 2 h followed by the addition of 10 μl of protein G-Sepharose 4B (Sigma) and further incubation at room temperature for 1 h. Immune complexes were collected by centrifugation at 13,000 × *g* at room temperature for 5 min and were washed three times in 0.3 ml of Radioimmune Precipitation Buffer and were finally resuspended in 1× Solubilization Buffer (10% β-mercaptoethanol (v/v), 2% SDS (w/v), 30% glycerol (v/v), 0.025% bromphenol blue (w/v), 50 mM Tris-HCl, pH 6.8; 60 μl). Samples were boiled for 5 min and then loaded onto 10% polyacrylamide gels, analyzed by SDS-PAGE, and thereafter electroblotted onto PVDF membranes essentially as described previously (12). Electroblots were then exposed to Eastman Kodak X-Omat XAR film to detect ^{32}P-labeled proteins. Thereafter blots were subjected to PhosphorImager analysis, and the intensities of phosphorylation relative to basal phosphorylation were determined and were expressed in arbitrary units of intensity relative to basal levels. In parallel experiments, cells were incubated under identical conditions in the absence of [^{32}P]orthophosphate. HAmIP and HAmIP^{S357A} receptors were immunoprecipitated, and immunoblots were screened using the anti-HA 3F10 horseradish peroxidase-conjugated antibody (1:500) to check for quantitative recovery of each receptor type. Immunoreactive proteins were visualized using the chemiluminescence detection system (12).

Co-immunoprecipations of the mIP and Its Associated G Proteins—HEK.HAmIP and HEK.HAmIP^{S357A} cells were transiently co-transfected with the respective pCMV·Gα plasmids encoding Gα_s, Gα_i, and Gα_q (25 μg/10-cm dish) and pADVA (10 μg/10-cm dish). Approximately 48 h post-transfection, cells were either preincubated for 10 min with 10 μM H-89 or, as a control, with an equivalent volume of the vehicle HBS at 37 °C in 5% CO_2 prior to stimulation with 1 μM cicaprost for 10 min at 37 °C in 5% CO_2. Reactions were terminated, and HA-tagged IP receptors were immunoprecipitated using the anti-HA 101R antibody (1:300), blotted, and analyzed essentially as described previously (12). Samples were resuspended in 1× Solubilization Buffer, boiled for 5 min, then analyzed by SDS-PAGE on 10% polyacrylamide gels, and thereafter electroblotted onto PVDF membranes. Membranes were then screened by immunoblot analysis using the appropriate Gα_s (K-20) (1:3000), G$\alpha_{q/11}$ (C-19) (1:3000), or G$\alpha_{i\text{-}1}$ (I-20) (1:500) antisera where horseradish peroxidase-conjugated goat anti-rabbit IgG (1:3000) was the secondary antibody used in each case. Immunoreactive proteins were visualized using the chemiluminescence detection system according to the manufacturer's recommendations.

Data Analyses

Statistical analysis was carried out using the unpaired Student's *t* test using GraphPad Prism Version 2.0 (GraphPad Software Inc., San Diego, CA). *p* values of less than or equal to 0.05 were considered to indicate a statistically significant difference.

RESULTS

Mouse Prostacyclin Receptor G Protein Coupling in Response to Adenylyl Cyclase Activation—In the current study we sought to investigate the specificity of G protein:effector coupling by the mIP and to define the mechanism(s) whereby the mIP may couple to more than one G protein:effector system. In addition, as a comparative control, we investigated signaling by the β_2AR, which has been reported to switch coupling from Gα_s to Gα_i in a PKA-dependent mechanism (23). Thus, our studies were performed in HEK 293 cells stably overexpressing the mIP (HEK.mIP cells), in MEL cells that endogenously express mIP, and in HEK.β_2AR cells stably overexpressing the human β_2AR (12). Initially radioligand binding assays established mIP expression levels in HEK.mIP cells and in MEL cells and β_2AR expression levels in HEK.β_2AR cells (Table I). Thereafter agonist-induced cAMP generation was determined in HEK.mIP cells (Fig. 1*A*) and in MEL cells (Fig. 1*B*) or in HEK.β_2AR cells (Fig. 1*C*) in response to stimulation of cells with the selective IP agonist cicaprost or the β_2AR agonist isoproterenol in the absence or presence of the diterpene forskolin to detect Gα_i coupling should it occur. Stimulation of HEK.mIP ($p < 0.0001$) and MEL ($p < 0.0001$) cells resulted in significant increases in cAMP generation consistent with mIP coupling to Gα_s. Whereas incubation of cells with forskolin resulted in agonist-

TABLE I
Radioligand binding assays

Cell type	[^{3}H]Iloprost bound[a]
	pmol mg^{-1} protein
HEK.mIP	3.28 ± 0.22
MEL	0.55 ± 0.02
HEK.mIP^{SSLC}	3.43 ± 0.47
HEK.HAmIP isolate 1	2.37 ± 0.12
HEK.HAmIP isolate 2	1.56 ± 0.21
HEK.HAmIP^{S357A}	1.57 ± 0.24
HEK 293	0.01 ± 0.001
Cell type	**[^{3}H]CGP-12177 bound[b]**
	fmol mg^{-1} protein
HEK.β_2AR	92.2 ± 5.0
HEK 293	15.0 ± 1.2

[a] Radioligand binding assays were carried out on membrane fractions of MEL cells, HEK 293 cells, or HEK 293 cells stably overexpressing either mIP (HEK.mIP cells), mIP^{SSLC} (HEK.mIP^{SSLC} cells), HA-tagged mIP (HEK.HAmIP isolates 1 and 2), or HA-tagged mIP^{S357A} (HEK.HAmIP^{S357A}) in the presence of 4 nM [^{3}H]iloprost.

[b] Radioligand binding assays were carried out on whole HEK 293 cells or on HEK 293 cells stably overexpressing the β_2AR (HEK.β_2AR cells) in the presence of 25 nM [^{3}H]CGP-12177. Data are presented as the mean ± S.E. (n = 4).

independent increases in cAMP generation, co-incubation with cicaprost and forskolin caused significant decreases in cAMP in both HEK.mIP ($p < 0.0001$) and MEL ($p < 0.0001$) cells. These results suggest that the mIP can couple to both Gα_s and Gα_i. Similar results were obtained upon examining cAMP generated by the β_2AR (Fig. 1*C*), consistent with previous reports that the β_2AR may couple to both Gα_s and Gα_i (23).

Preincubation of HEK.mIP (Fig. 2*A*) or HEK.β_2AR (Fig. 2*D*) cells with PTx abolished both mIP ($p < 0.001$) and β_2AR ($p < 0.001$) coupling to Gα_i. Whereas preincubation of either HEK.mIP (Fig. 2*B*) or HEK.β_2AR (Fig. 2*E*) cells with the PKA inhibitor H-89 prior to agonist stimulation had no effect on mIP- or β_2AR-induced cAMP generation, it abolished the mIP and β_2AR coupling to Gα_i (HEK.mIP, $p < 0.001$; HEK.β_2AR, $p < 0.001$). On the other hand, the PKC inhibitor GF 109203X (Fig. 2, *panels C* and *F*) had no significant effect on either Gα_s or Gα_i coupling by either the mIP (Fig. 2*C*, $p < 0.3988$) or the β_2AR (Fig. 2*F*, $p < 0.5257$).

To determine whether the mIP:Gα_i coupling is dependent on the concentration of ligand used for stimulation, HEK.mIP cells were stimulated with cicaprost (1 pM–1 μM) in the absence and presence of forskolin (Fig. 3*A*). mIP generated significant concentration-dependent increases in cAMP consistent with its coupling to Gα_s. However, in cells co-incubated with forskolin, 1 pM–1 nM cicaprost led to concentration-dependent augmentations of cAMP generation consistent with mIP coupling to Gα_s; however, at the higher cicaprost concentrations (>1 nM), cicaprost led to a concentration-dependent reduction in cAMP generation indicative of mIP coupling to Gα_i. In the presence of PTx, cicaprost led to concentration-dependent increases in cAMP generation in the presence (Fig. 3*B*) and absence of forskolin (data not shown) over the complete range of cicaprost concentrations (1 pM–1 μM). Moreover, in the presence of H-89, cicaprost resulted in concentration-dependent increases in cAMP generation in the presence (Fig. 3*B*) and absence of forskolin (data not shown) over the complete range of cicaprost concentrations providing further evidence that Gα_i coupling by mIP is dependent on PKA activation status.

Mouse Prostacyclin Receptor Coupling to PLC—We extended these studies to investigate the mechanism whereby the G_s-coupled mIP may also couple to the Gα_q:PLC effector system (12). Stimulation of cells with cicaprost resulted in a significant increase in IP_3 generation in HEK.mIP cells compared with control, nontransfected HEK 293 cells (Figs. 4*A* and 10*A*, $p < 0.0009$). Preincubation of HEK.mIP cells with PTx or GF 109203X had no significant effect on IP_3 generation (PTx, $p > 0.911$; GF 109203X, $p > 0.668$); however, preincubation with H-89 significantly decreased cicaprost-induced IP_3 generation ($p < 0.005$). Because the levels of cicaprost-stimulated IP_3 were quite low (1.56 ± 0.13-fold increase in IP_3 in response to 1 μM cicaprost), HEK.mIP cells were transiently co-transfected with Gα_q to increase the levels of measurable IP_3 (Fig. 4*B*). Overexpression of Gα_q was confirmed by Western blot analysis using anti-Gα_q-specific antisera (Fig. 4*C*). The presence of Gα_q augmented ($p < 0.002$) and led to a significant increase in cicaprost-induced IP_3 generation (Fig. 4*B*), and cicaprost-induced IP_3 generation in the presence of Gα_q was not affected by preincubation with either PTx ($p > 0.812$) or GF 109203X ($p > 0.896$). However, preincubation with H-89 abolished cicaprost-mediated IP_3 production (Fig. 4*B*, $p < 0.0001$) such that the levels of IP_3 generation were not significantly different to those levels generated in control, nontransfected HEK 293 cells following cicaprost stimulation ($p > 0.25$).

To extend these studies, we also investigated cicaprost-induced PLC activation by monitoring mobilization of $[Ca^{2+}]_i$. Consistent with previous studies (12), stimulation of HEK.mIP cells with cicaprost resulted in efficient transient rises in $[Ca^{2+}]_i$ mobilization (Fig. 5*A*). Preincubation of HEK.mIP cells with PTx (Fig. 5*B*) prior to stimulation with cicaprost had no significant effect on $[Ca^{2+}]_i$ mobilization ($p > 0.627$). Consistent with this, transient overexpression of the carboxyl-terminal residues (amino acid residues 459–689) of βARK1 (25) to sequester G$\beta\gamma$ subunits had no significant effect on cicaprost-induced $[Ca^{2+}]_i$ mobilization (Fig. 5*C*, $p > 0.32$). Overexpression of the carboxyl-terminal residues of βARK1 was confirmed by Western blot analysis (Fig. 5*D*). Preincubation of HEK.mIP cells with the PKC inhibitor GF 109203X had no significant effect on $[Ca^{2+}]_i$ mobilization by the mIP (Fig. 5*E*, $p > 0.24$). In contrast, preincubation of HEK.mIP cells with H-89 resulted in near complete inhibition of cicaprost-induced $[Ca^{2+}]_i$ mobilization (Fig. 5*F*, $p < 0.001$).

Thereafter to confirm that the source of cicaprost-induced $[Ca^{2+}]_i$ mobilization is derived from PLC/IP_3-regulated intracellular Ca^{2+}stores, we examined the effect of the PI-PLC inhibitor U73122 and, as a control, the phosphatidylcholine-specific phospholipase C inhibitor D-609 (31, 32) on cicaprost-induced $[Ca^{2+}]_i$ mobilization. Preincubation of HEK.mIP cells with U73122 abolished $[Ca^{2+}]_i$ mobilization by the mIP (Fig. 6*B*, $p < 0.0001$), whereas preincubation of the cells with D-609 had no significant effect on cicaprost-induced $[Ca^{2+}]_i$ mobilization (Fig. 6*C*, $p > 0.07$). As an additional control, preincubation of HEK.mIP cells with U73122 did not affect ionomycin-induced $[Ca^{2+}]_i$ mobilization ensuring that U73122 did not affect the general measurement of $[Ca^{2+}]_i$ mobilization in Fura2/AM-preloaded cells *per se* ($p < 0.001$, data not shown).

Whole Cell Phosphorylations of the mIP—To establish whether the mIP may be subject to cicaprost-induced PKA phosphorylation, whole cell phosphorylations of the mIP were investigated in HEK 293 cells stably overexpressing an amino-terminal extracellular HA epitope-tagged mIP (HEK.HAmIP cells). Consistent with previous reports (12, 33) and Table I, the presence of the HA epitope tag did not affect the ligand binding characteristics or cell signaling properties of mIP (data not shown). Initially the specificity of the anti-HA 101R antiserum to immunoprecipitate HAmIP from HEK.HAmIP cells and not from HEK 293 cells (Fig. 7*C*) or HEK.mIP cells (data not shown) was confirmed. Short term exposure of the Western blot revealed the presence of two distinct immunoreactive bands (Fig. 7*C*, *lane 1*), one between 46 and 66 kDa and the other

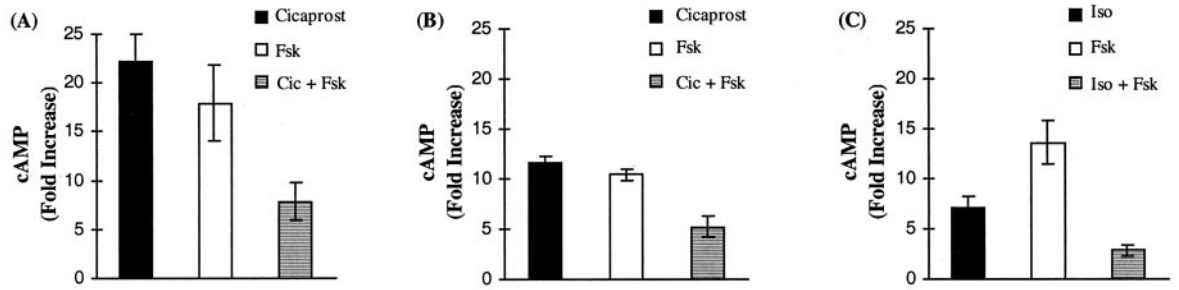

FIG. 1. **Agonist-induced cAMP generation.** HEK.mIP cells (*panel A*) and MEL cells (*panel B*) were stimulated with either 1 μM cicaprost, 10 μM forskolin (*Fsk*), or 1 μM cicaprost plus 10 μM forskolin (*Cic + Fsk*). Alternatively, HEK.β_2AR cells (*panel C*) were stimulated with either 10 μM isoproterenol (*Iso*), 10 μM forskolin (*Fsk*), or 10 μM isoproterenol plus 10 μM forskolin (*Iso + Fsk*). In each case, basal cAMP levels were determined by exposing the cells to the vehicle under identical reaction conditions. Levels of cAMP produced in ligand-stimulated cells relative to basal cAMP levels were expressed as -fold stimulation of basal (-fold increase in cAMP ± S.E., $n = 4$). Basal levels of cAMP generation in HEK.mIP cells and in MEL cells were 0.71 ± 0.04 pmol/mg of cell protein ($n = 4$) and 0.98 ± 0.06 pmol/mg of cell protein ($n = 4$), respectively.

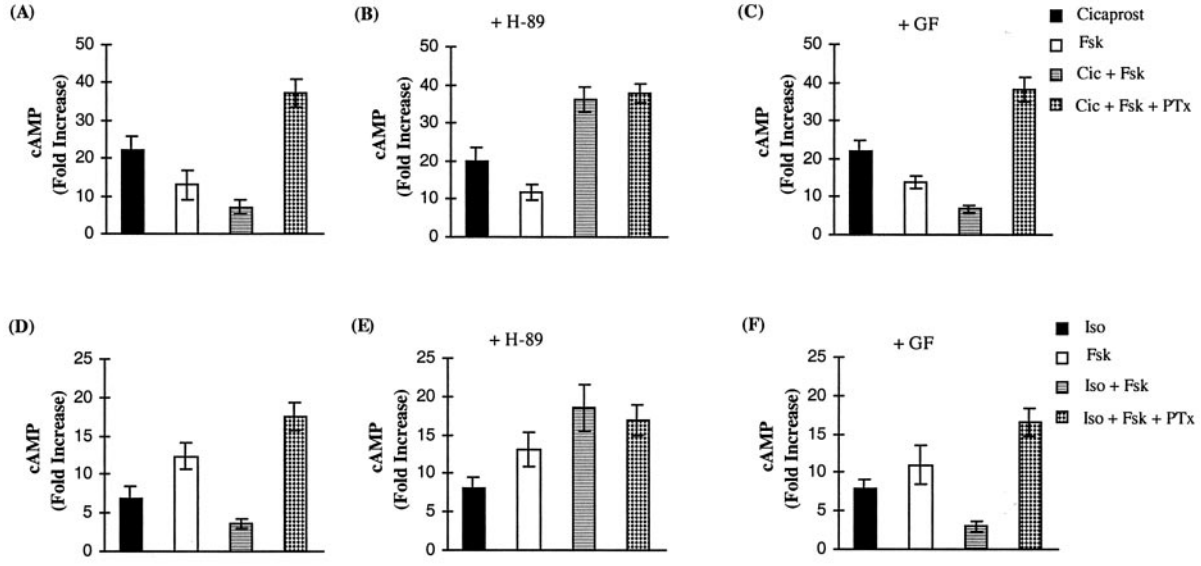

FIG. 2. **The effect of kinase inhibitors on cicaprost-induced cAMP generation.** HEK.mIP cells (*panel A*) were stimulated with either 1 μM cicaprost, 10 μM forskolin (*Fsk*), or 1 μM cicaprost plus 10 μM forskolin (*Cic + Fsk*) or were preincubated with PTx (50 ng/ml, 16 h) prior to stimulation with 1 μM cicaprost plus 10 μM forskolin (*Cic + Fsk + PTx*). HEK.β_2AR cells (*panel D*) were stimulated with either 10 μM isoproterenol (*Iso*), 10 μM forskolin (*Fsk*), or 10 μM isoproterenol plus 10 μM forskolin (*Iso + Fsk*) or were preincubated with PTx (50 ng/ml, 16 h) prior to stimulation with 10 μM isoproterenol plus 10 μM forskolin (*Iso + Fsk + PTx*). Alternatively HEK.mIP cells (*panels B* and *C*) or HEK.β_2AR cells (*panels E* and *F*) were preincubated for 10 min with 10 μM H-89 (*panels B* and *E*) or 50 nM GF 109203X (*GF*) (*panels C* and *F*) prior to stimulation with ligand as outlined in *panels A* and *D*, respectively. In each case, basal cAMP levels were determined by exposing the cells to the vehicle HBS under identical reaction conditions. Levels of cAMP produced in ligand-stimulated cells relative to basal cAMP levels were expressed as -fold stimulation of basal (-fold increase in cAMP ± S.E., $n = 4$). Basal levels of cAMP generation in HEK.mIP cells and in HEK.β_2AR cells were 0.81 ± 0.03 pmol/mg of cell protein ($n = 4$) and 0.74 ± 0.05 pmol/mg of cell protein ($n = 4$), respectively.

between 36 and 46 kDa, corresponding to the glycosylated and nonglycosylated forms of mIP, respectively (12, 33), which appeared as a single broad band of 36–66 kDa following prolonged exposure (data not shown). In ^{32}P metabolically labeled cells, cicaprost resulted in phosphorylation of a broad protein band of 36–66 kDa, corresponding to the immunoprecipitated HAmIP in HEK.HAmIP cells (Fig. 7*A*, *lane 2*). In contrast, no phosphorylation of mIP occurred in vehicle-treated, nonstimulated HEK.HAmIP cells (Fig. 7*A*, *lane 1*) or in cicaprost-stimulated HEK 293 control cells (Fig. 7*A*, *lane 5*). Whereas preincubation of HEK.HAmIP cells with the PKC inhibitor GF 109203X did not significantly affect cicaprost-mediated mIP phosphorylation (Fig. 7*A*, *lane 3*; $p > 0.05$), preincubation of HEK.HAmIP cells with the PKA inhibitor H-89 (Fig. 7*B*, *lane 4*) abolished cicaprost-induced HAmIP phosphorylation ($p < 0.05$).

The Role of the C-tail of the mIP in Receptor:G Protein Coupling—It has previously been established that the isoprenylation-defective mIP^{SSLC}, in which the critical Cys^{414} of mIP was mutated to Ser^{414} to generate mIP^{S414SLC}, cannot couple to Gα_s to mediate cAMP increases and cannot efficiently couple to Gα_q:PLC activation (12) implying that the C-tail of the mIP may be important in receptor:G protein coupling. Thus, we sought to investigate whether the isoprenylation-defective mIP^{SSLC} can couple to Gα_i. Consistent with previous studies (12), HEK.mIP^{SSLC} cells exhibited a significantly impaired ability to generate cicaprost-mediated cAMP generation compared with HEK.mIP cells (Fig. 8, compare *panel A* to *panel C*). In fact the levels of cicaprost-induced cAMP generation in HEK.mIP^{SSLC} cells were not significantly different from that produced by the control, nontransfected HEK 293 cells over the range of 1 pM–100 nM cicaprost (data not shown), but at 1 μM cicaprost a small, although significant, increase in cAMP generation was observed in HEK.mIP^{SSLC} cells (Fig. 8*A*, $p < 0.05$). Moreover, in the presence of forskolin, cicaprost (1 μM) did not result in a diminution of cAMP levels, indicative of Gα_i coupling, in HEK.mIP^{SSLC} cells ($p > 0.65$) but rather showed a marginal augmentation in cAMP generation (Fig. 8*A*). H-89 had no effect on the level of Gα_s or Gα_i coupling by mIP^{SSLC} (Fig. 8*B*), but consistent with previous data (Fig. 2*B*) it signif-

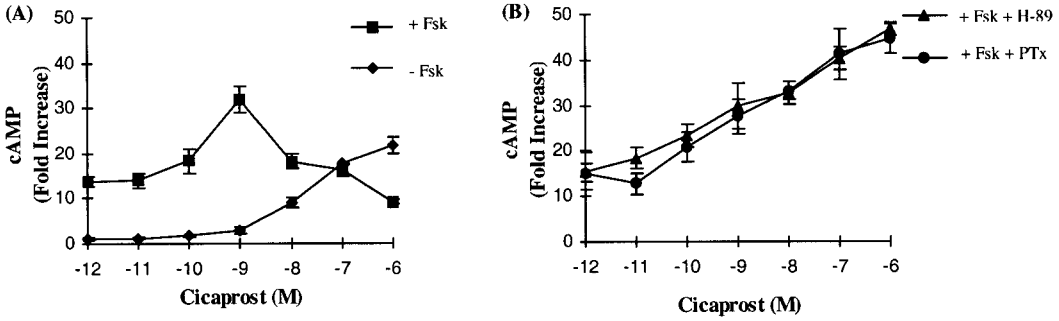

FIG. 3. **The effect of cicaprost concentration on mIP-induced cAMP generation.** HEK.mIP cells were stimulated with cicaprost (1 pM–1 μM) in the presence (+) or absence (−) of 10 μM forskolin (*Fsk*) (*panel A*). Alternatively, HEK.mIP cells were preincubated with PTx (50 ng/ml, 16 h) or with H-89 (10 μM, 10 min) prior to stimulation with 1 pM–1 μM cicaprost in the presence of 10 μM forskolin (*panel B*). In each case, basal cAMP levels were determined by exposing the cells to the vehicle under identical reaction conditions. Levels of cAMP produced in ligand-stimulated cells relative to basal cAMP levels were expressed as -fold stimulation of basal (-fold increase in cAMP ± S.E., $n = 4$). The basal level of cAMP generation in HEK.mIP cells was 0.79 ± 0.04 pmol/mg of cell protein ($n = 4$).

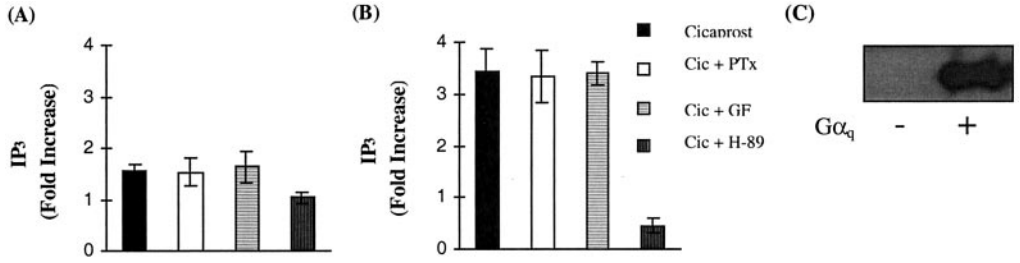

FIG. 4. **The effect of kinase inhibitors on cicaprost-induced IP_3 generation in HEK.mIP cells.** HEK.mIP cells (*panel A*) and HEK.mIP cells transiently co-transfected with $G\alpha_q$ (*panel B*) were stimulated with 1 μM cicaprost or were preincubated with PTx (50 ng/ml, 16 h), GF 109203X (*GF*) (50 nM, 10 min), or H-89 (10 μM, 10 min) prior to stimulation with 1 μM cicaprost. In each case, basal IP_3 levels were determined by exposing the cells to the vehicle HBS under identical reaction conditions. Levels of IP_3 produced in ligand-stimulated cells relative to vehicle-treated cells (basal IP_3) were expressed as -fold stimulation of basal (-fold increase in IP_3 ± S.E., $n = 4$). *Panel C* represents a typical Western blot confirming overexpression of $G\alpha_q$ in HEK.mIP cells (75 μg of total cellular protein analyzed). Basal levels of IP_3 generation in HEK.mIP cells and in HEK.mIP cells transiently co-transfected with $G\alpha_q$ were 0.36 ± 0.04 pmol/mg of cell protein ($n = 4$) and 0.49 ± 0.04 pmol/mg of cell protein ($n = 4$), respectively.

icantly impaired mIP coupling to $G\alpha_i$ (Fig. 8*D*). To exclude the possibility that the inability of the mIP^{SSLC} to generate cAMP is not due to low levels of IP, radioligand binding assays were carried out on HEK.mIP^{SSLC} membranes (Table I). No significant differences were observed between the levels of mIP expression in HEK.mIP and HEK.mIP^{SSLC} cells ($p > 0.0985$).

Computational analysis of the C-tail region of the IP revealed a putative PKA phosphorylation site in the mIP sequence where Ser^{357} represents the predicted target residue for PKA phosphorylation (34). Thus, to determine the importance of this potential PKA phosphorylation motif, site-directed mutagenesis was used to generate mIP^{S357A}, a variant of mIP in which Ser^{357} was converted to Ala^{357}, thereby destroying the putative PKA phosphorylation site within the C-tail of mIP. Stable cell lines overexpressing the epitope-tagged (HA) mIP^{S357A} (HEK.HAmIP^{S357A}) were established and characterized by radioligand binding (Table I). Whereas through transient expression studies it was established that mutation of Ser^{357} did not affect the ligand binding characteristics of the mIP^{S357A} compared with the wild type mIP, the level of mIP^{S357A} expression in HEK.HAmIP^{S357A} cells was appreciably lower than that of mIP expressed in HEK.mIP or in HEK-.HAmIP cells (Table I). Thus, to ensure that any potential difference in the signaling behavior of the mIP^{S357A} when compared with the mIP may not be due to simple differences in the relative levels of the respective receptor expression, for further studies we chose to use a second pure clonal cell line or isolate of the HEK.HAmIP cells (HEK.HAmIP isolate 2) that exhibited similar levels of mIP expression to that of the HEK.HAmIP^{S357A} cells (Table I). Both the HEK.HAmIP and HEK.HAmIP^{S357A} cells showed significant cicaprost-mediated, concentration-dependent increases in cAMP generation (Fig. 9*A*). Moreover, co-transfection of cells with $G\alpha_s$ (Fig. 9*B*) significantly augmented cAMP generation in HEK.HAmIP cells ($p < 0.003$) and in HEK.HAmIP^{S357A} cells ($p < 0.0001$) where $G\alpha_s$ overexpression was confirmed by Western blot analysis (Fig. 9*B*, *inset*). However, whereas mIP^{S357A} exhibited efficient $G\alpha_s$ coupling ($p < 0.001$) unlike that of the mIP isolates, it did not exhibit $G\alpha_i$ coupling as evidenced by its failure to reduce, but rather augmented, cAMP levels in cells co-stimulated with cicaprost plus forskolin when compared with cells incubated with forskolin alone (Fig. 9*C*). cAMP generation by the mIP^{S357A} was not affected by the presence of H-89 (Fig. 9*D*) or GF 109203X (data not shown).

Next the ability of mIP^{S357A} to couple to $G\alpha_q$ and PLC activation was examined. HEK.HAmIP cells produced a concentration-dependent increase in IP_3 generation upon stimulation with 1 nM–10 μM cicaprost (Fig. 10*A*, $p < 0.001$ at 10 μM cicaprost). In contrast, neither the HEK.HAmIP^{S357A} or the nontransfected HEK 293 cells showed any significant increases in IP_3 even at the highest concentration used ($p > 0.249$ at 10 μM and $p > 0.314$ at 10 μM, respectively). Moreover, co-transfection of cells with $G\alpha_q$ did not augment cicaprost-mediated IP_3 generation in HEK.HAmIP^{S357A} cells (data not shown). Stimulation of both the mIP and the mIP^{S357A} did lead to significant increases in $[Ca^{2+}]_i$ mobilization (Fig. 10*B*); however, the level of $[Ca^{2+}]_i$ mobilization by the mIP^{S357A} was significantly less than that of the mIP ($p < 0.003$) and was only marginally greater than that mobilized in nontransfected HEK 293 cells in response to cicaprost (Ref. 12 and data not shown).

Whole Cell Phosphorylations of the mIP^{S357A}—Whole cell phosphorylations in HEK.HAmIP^{S357A} cells (Fig. 7*B*) con-

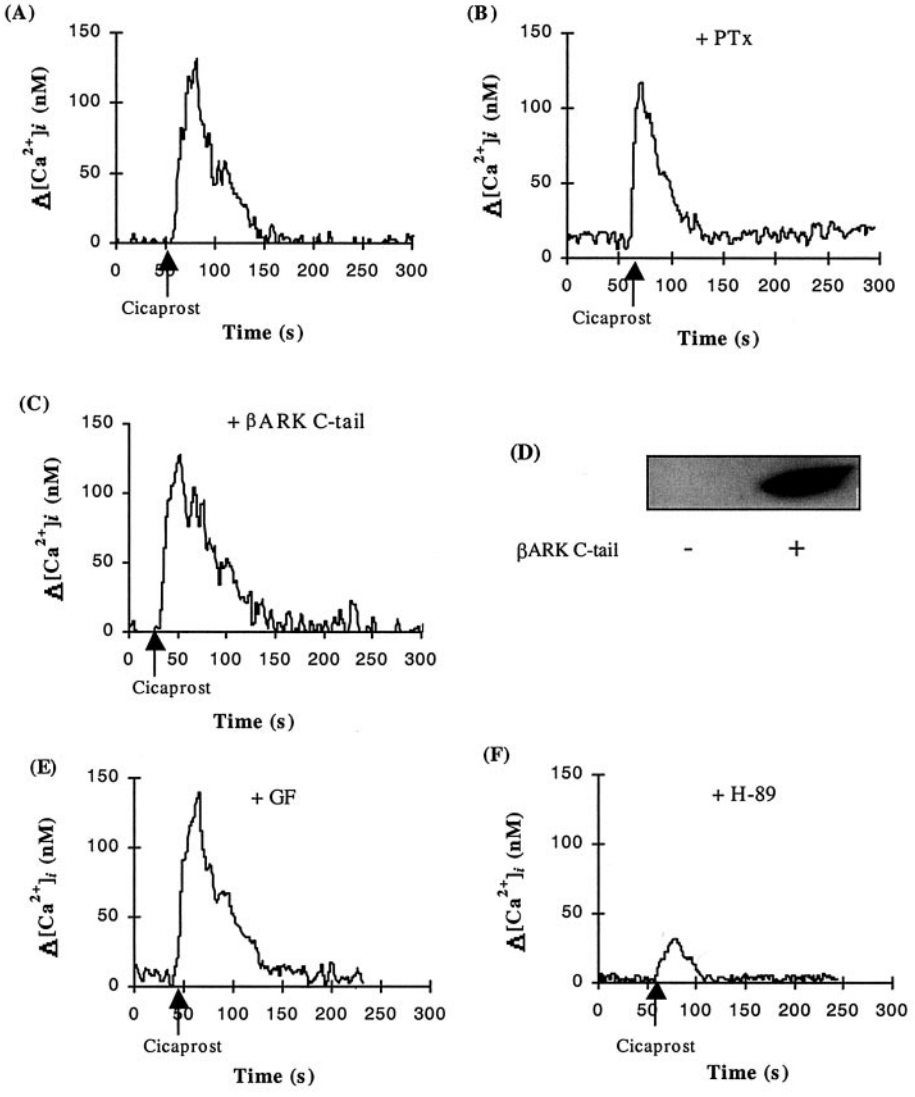

FIG. 5. **Effect of protein kinase inhibitors on $[Ca^{2+}]_i$ mobilization in HEK.mIP cells.** HEK.mIP cells (*panel A*) or HEK.mIP cells preincubated with PTx (50 ng/ml, 16 h) (*panel B*) were stimulated with 1 μM cicaprost. HEK.mIP cells were transiently co-transfected with the cDNA for the βARK1 C-tail (residues 459–689) (*panel C*) or were preincubated for 10 min with 50 nM GF 109203X (*GF*) (*panel E*) or 10 μM H-89 (*panel F*) prior to stimulation with 1 μM cicaprost. In each case, cicaprost was added at the time indicated by the *arrows*. Data were calculated as changes in intracellular Ca^{2+} mobilized ($\Delta[Ca^{2+}]_i \pm$ S.E., nM) as a function of time following ligand stimulation, and the data presented are representative of at least three independent experiments. Actual changes in $[Ca^{2+}]_i$ mobilized were as follows: *panel A*, $\Delta[Ca^{2+}]_i = 130 \pm 10.9$ nM; *panel B*, $\Delta[Ca^{2+}]_i = 121 \pm 14.4$ nM; *panel C*, $\Delta[Ca^{2+}]_i = 143 \pm 3.58$ nM, *panel E*: $\Delta[Ca^{2+}]_i = 126 \pm 9.4$ nM; *panel F*, $\Delta[Ca^{2+}]_i = 27.3 \pm 5.57$ nM. Aliquots (75 μg/lane) of HEK.mIP cells (−) or HEK.mIP cells transiently co-transfected with the cDNA for the βARK1 C-tail (+) were screened by Western blot analysis using the anti-βARK1 antibody as described under "Experimental Procedures" (*panel D*). These data are representative of three independent experiments.

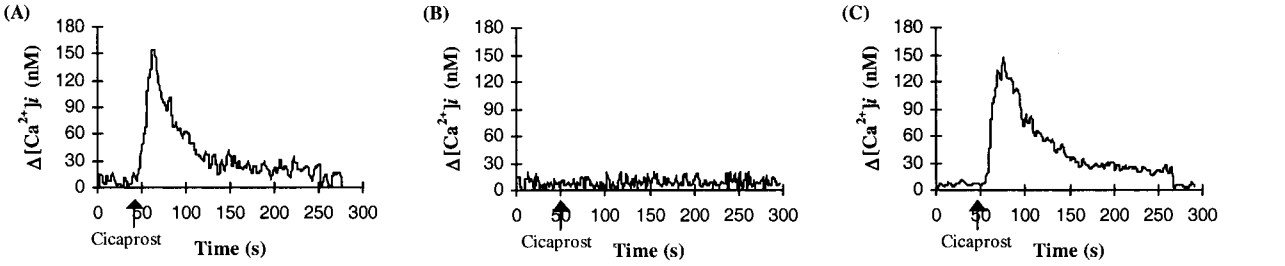

FIG. 6. **Effect of PLC inhibitors on $[Ca^{2+}]_i$ mobilization in HEK.mIP cells.** HEK.mIP cells (*panel A*) or HEK.mIP cells preincubated for 5 min with 1 μM U73122 (*panel B*) or 10 μM D-609 (*panel C*) were stimulated with 1 μM cicaprost where cicaprost was added at the times indicated by the *arrows*. Data were calculated as changes in intracellular Ca^{2+} mobilized ($\Delta[Ca^{2+}]_i \pm$ S.E., nM) as a function of time following ligand stimulation and are representative of at least three independent experiments. Actual changes in $[Ca^{2+}]_i$ mobilized were as follows: *panel A*, $\Delta[Ca^{2+}]_i = 143 \pm 1.84$ nM; *panel B*, $\Delta[Ca^{2+}]_i = 6.67 \pm 3.33$ nM; *panel C*, $\Delta[Ca^{2+}]_i = 133 \pm 11.9$ nM.

firmed that $HAmIP^{S357A}$ did undergo increased phosphorylation, represented as a broad phosphoprotein band of 36–66 kDa, in response to stimulation with cicaprost (Fig. 7*B*, compare *lanes 1* and *2*). However, the level of $HAmIP^{S357A}$ phosphorylation was not significantly different from that observed in HEK 293 cells (Fig. 7*A*, *lane 5*; $p > 0.05$) but was substantially less when compared with that of the HAmIP (Fig. 7, compare *panel A*, *lane 2* to *panel B*, *lane 2*; $p < 0.05$) despite the fact that $HAmIP^{S357A}$ was expressed at levels similar to that of the HAmIP (Fig. 7*C*, *lanes 1* and *2*; Table I). Moreover, preincubation of $HEK.HAmIP^{S357A}$ cells with GF 109203X or H-89 (Fig. 7*B*, *lanes 3* and *4*, respectively) had no effect on the level of mIP^{S357A} phosphorylation in cicaprost-stimulated cells.

mIP and mIP^{S357A} Receptor:G Protein Interactions—To investigate the G protein interactions of the mIP and the mIP^{S357A} more closely, HEK.HAmIP (Fig. 11*A*) and $HEK.HA\text{-}mIP^{S357A}$ (Fig. 11*B*) cells were transiently transfected with the cDNA encoding the α subunit of $G\alpha_s$ (Fig. 11, *panels A* and *B*, *lanes 1* and *2*), $G\alpha_i$ (Fig. 11, *panels A* and *B*, *lanes 3* and *4*), or $G\alpha_q$ (Fig. 11, *panels A* and *B*, *lanes 5* and *6*). Receptor:G protein interactions were examined by immunoprecipitating the HAmIP or $HAmIP^{S357A}$ receptor using

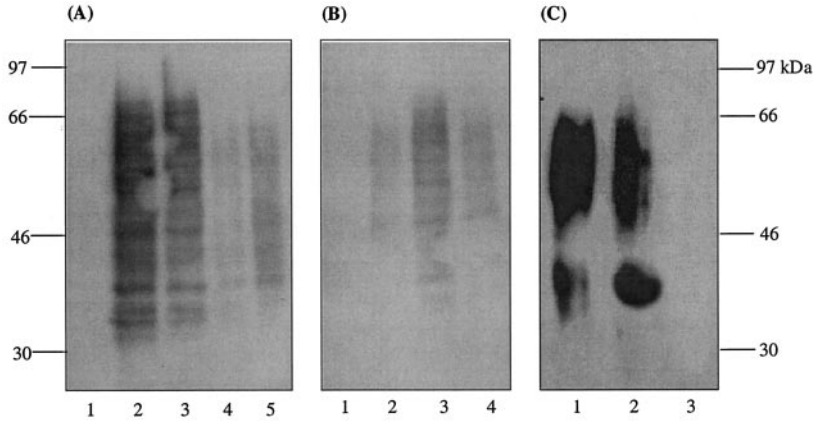

FIG. 7. **Cicaprost-induced phosphorylation of the mIP and mIP^{S357A}.** *Panels A* and *B*, HEK.HAmIP isolate 2 cells (*panel A*, *lanes 1–4*), HEK.HAmIP^{S357A} cells (*panel B*), or control HEK 293 cells (*panel A*, *lane 5*) metabolically labeled with [^{32}P]orthophosphate were incubated for 10 min with the vehicle HBS (*panels A* and *B*, *lane 1*) or were stimulated for 10 min with 1 μM cicaprost (*panels A* and *B*, *lanes 2* and *5*). Additionally, HEK.HAmIP isolate 2 cells and HEK.HAmIP^{S357A} cells were preincubated with 50 nM GF 109203X (*panels A* and *B*, *lane 3*) or 10 μM H-89 (*panels A* and *B*, *lane 4*) for 10 min prior to stimulation with 1 μM cicaprost for 10 min. Thereafter HA epitope-tagged IP receptors were immunoprecipitated using the anti-HA antibody 101R. Immunoprecipitates were resolved by SDS-PAGE, electroblotted onto PVDF membranes, and then exposed to Xomat XAR-5 film (Kodak) for 8–10 days. Thereafter blots were subjected to PhosphorImage analysis, and the intensities of cicaprost-mediated mIP and mIP^{S357A} phosphorylation relative to basal phosphorylation in the presence of HBS were determined and expressed in arbitrary units as follows: mIP: 1 μM cicaprost, 11.2-fold; 1 μM cicaprost plus 50 nM GF 109203X, 9.1-fold; 1 μM cicaprost plus 10 μM H-89, 1-fold; mIP^{S357A}: 1 μM cicaprost, 1.51-fold; 1 μM cicaprost plus 50 nM GF 109203X, 2.8-fold; 1 μM cicaprost plus 10 μM H-89, 1.9-fold; HEK 293: 1 μM cicaprost, 1.23-fold. *Panel C*, HEK.HAmIP isolate 2 (*lane 1*), HEK.HAmIP^{S357A} (*lane 2*), or control HEK 293 (*lane 3*) cells were subjected to immunoprecipitation using the anti-HA antibody 101R, and immunoprecipitates were resolved by SDS-PAGE and electroblotted onto PVDF membranes. Membranes were screened using the anti-HA 3F10 horseradish peroxidase-conjugated antibody, and immunoreactive bands were visualized by chemiluminescence detection. The positions of the molecular weight markers (kDa) are indicated to the *left* and *right* of *panels A* and *C*, respectively. Data presented are representative of three independent experiments.

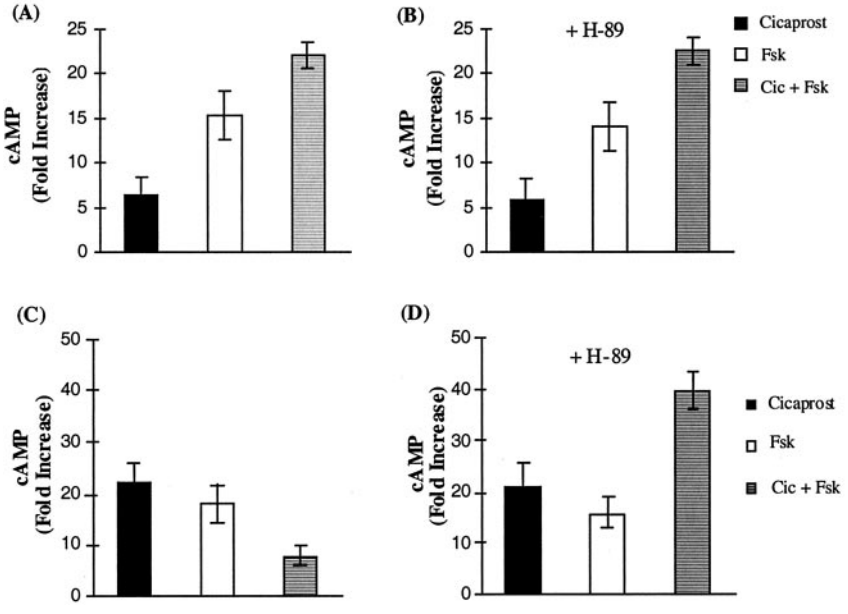

FIG. 8. **Cicaprost-induced cAMP generation by the mIP^{SSLC}.** HEK.mIP^{SSLC} (*panels A* and *B*) or HEK.mIP (*panels C* and *D*) cells preincubated for 10 min in the absence (*panels A* and *C*) or presence of 10 μM H-89 (*panels B* and *D*) were stimulated with either 1 μM cicaprost, 10 μM forskolin (*Fsk*), or 1 μM cicaprost plus 10 μM forskolin (*Cic + Fsk*). In each case, basal cAMP levels were determined by exposing the cells to the vehicle under identical reaction conditions. Levels of cAMP produced in ligand-stimulated cells relative to basal cAMP levels were expressed as -fold stimulation of basal (-fold increase in cAMP ± S.E., $n = 4$). Basal levels of cAMP generation in HEK.mIP^{SSLC} cells and in HEK.mIP cells were 0.83 ± 0.04 pmol/mg of cell protein ($n = 4$) and 0.71 ± 0.04 pmol/mg of cell protein ($n = 4$), respectively.

the anti-HA 101R antisera followed by screening the immunoprecipitates for co-precipitation of the respective Gα subunit using anti-Gα-specific antisera. Whereas nonstimulated, vehicle (HBS)-treated cells showed no receptor:G protein interaction (data not shown), stimulation of both HEK.HAmIP and HEK.HAmIP^{S357A} cells with cicaprost (1 μM) for 10 min permitted co-precipitation of Gα_s. However, whereas stimulation of HEK.HAmIP cells with cicaprost resulted in co-precipitation of HAmIP with Gα_i and Gα_q, precipitation of neither Gα_i nor Gα_q along with HAmIP^{S357A} was observed. The presence of HAmIP and HAmIP^{S357A} in the immunoprecipitates was confirmed by screening the blots with the anti-HA 3F10 horseradish peroxidase-conjugated antibody (data not shown). Moreover, pretreatment of HEK.HAmIP cells with H-89 blocked co-precipitation of Gα_i (Fig. 11*C*, *lanes 3* and *4*) and Gα_q (Fig. 11*C*, *lanes 5* and *6*) but had no effect on co-precipitation of Gα_s along with HAmIP (Fig. 11*C*, *lanes 1* and *2*).

DISCUSSION

Prostacyclin is central to the regulation of vascular hemostasis and may also mediate other somewhat diverse cellular actions under both physiologic and pathophysiologic settings (3, 8, 35). Mice deficient in the IP exhibit altered pain perception and inflammatory reactions as well as exhibiting an impaired response to thrombotic stimuli (4). Whereas IP is primarily coupled to G_s-dependent adenylyl cyclase activation, ligand activation of multiple signaling pathways by IP agonists has been identified, such as in mouse BNu2cl3 mast cells (36), in mouse preadipocyte Ob1771 cells (37), in human erythroleu-

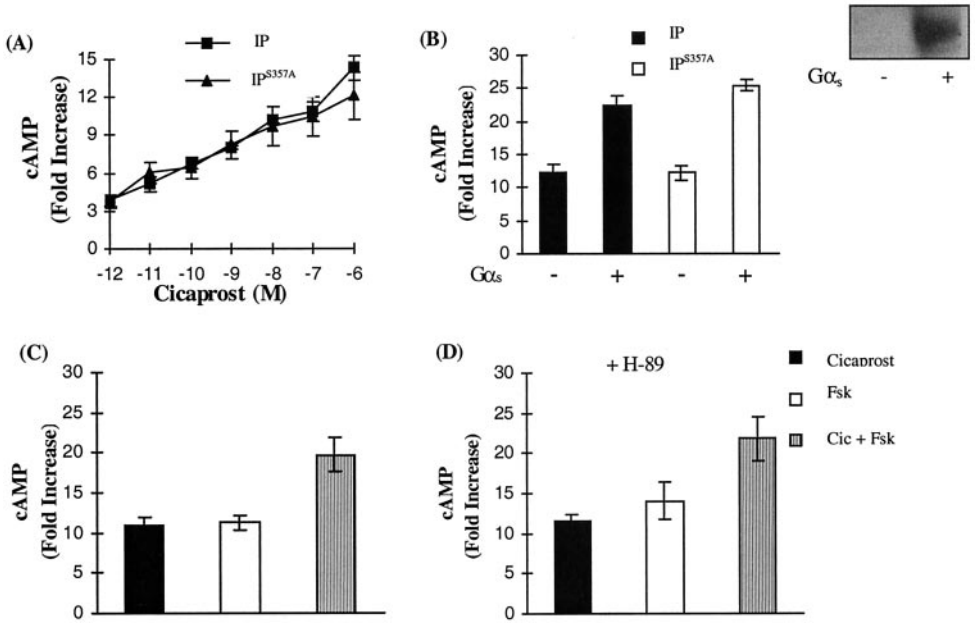

FIG. 9. **The effect of kinase inhibitors on cicaprost-induced cAMP generation by the mIP^{S357A}.** HEK.HAmIP isolate 2 (*IP*) and HEK.HAmIP^{S357A} (*IP^{S357A}*) cells were stimulated with 1 pM–1 μM cicaprost (*panel A*). Alternatively HEK.HAmIP isolate 2 (*IP*) and HEK.HAmIP^{S357A} (*IP^{S357A}*) cells that had been transiently co-transfected with either the vector pCMV5 (−) or with the cDNA for Gα_s (+) were stimulated with 1 μM cicaprost (*panel B*). The *inset* to *panel B* represents a typical Western blot confirming overexpression of Gα_s in HEK.HAmIP isolate 2 cells (75 μg of total cellular protein analyzed) and in HEK.HAmIP^{S357A} cells (data not shown). HEK.HAmIP^{S357A} cells (*panel C*) and HEK.HAmIP^{S357A} cells preincubated for 10 min with 10 μM H-89 (*panel D*) were stimulated with either 1 μM cicaprost, 10 μM forskolin (*Fsk*), or 1 μM cicaprost plus 10 μM forskolin (*Cic + Fsk*). In each case, basal cAMP levels were determined by exposing the cells to the vehicle HBS under identical reaction conditions. Levels of cAMP produced in ligand-stimulated cells relative to basal cAMP levels were expressed as -fold stimulation of basal (-fold increase in cAMP ± S.E., $n = 4$). Basal levels of cAMP generation in HEK.HAmIP isolate 2 (*IP*) and HEK.HAmIP^{S357A} (*IP^{S357A}*) cells were 0.53 ± 0.05 pmol/mg of cell protein ($n = 4$) and 0.79 ± 0.06 pmol/mg of cell protein ($n = 4$), respectively.

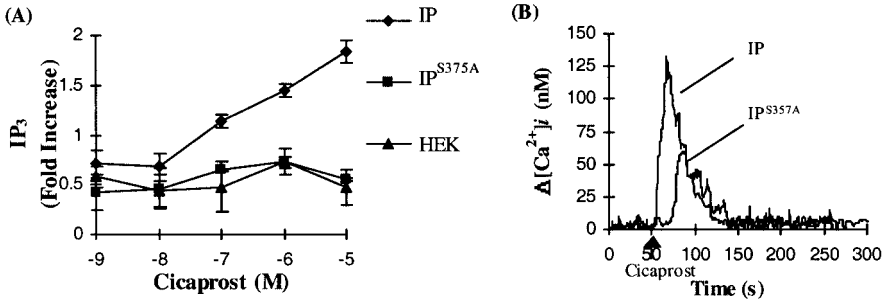

FIG. 10. **Cicaprost-induced IP_3 generation and $[Ca^{2+}]_i$ mobilization by the mIP^{S357A}.** *Panel A*, HEK.HAmIP isolate 2 (*IP*), HEK.HAmIP^{S357A} (*IP^{S357A}*), and HEK 293 (*HEK*) cells were stimulated with cicaprost (1 nM–10 μM), and the levels of IP_3 generation were measured (*panel A*). In each case, basal IP_3 levels were determined by exposing the cells to the vehicle HBS under identical reaction conditions. Levels of IP_3 produced in ligand-stimulated cells relative to basal levels were expressed as -fold stimulation of basal (-fold increase in IP_3 ± S.E., $n = 4$). Basal levels of IP_3 generation in HEK.HAmIP isolate 2 (*IP*) cells, in HEK.HAmIP^{S357A} (*IP^{S357A}*) cells, and in nontransfected HEK 293 (*HEK*) cells were 0.37 ± 0.03 pmol/mg of cell protein ($n = 4$), 0.39 ± 0.04 pmol/mg of cell protein ($n = 4$), and 0.29 ± 0.03 pmol/mg of cell protein ($n = 4$), respectively. *Panel B*, HEK.HAmIP isolate 2 (*IP*) and HEK.HAmIP^{S357A} (*IP^{S357A}*) were stimulated with 1 μM cicaprost, and $[Ca^{2+}]_i$ mobilization was measured where cicaprost was added at the time indicated by the *arrow* (*panel B*). Data were calculated as changes in intracellular Ca^{2+} mobilized ($\Delta[Ca^{2+}]_i$ ± S.E., nM) as a function of time following ligand stimulation, and data presented are representative of at least three independent experiments. Actual changes in $[Ca^{2+}]_i$ mobilized were as follows in *panel B*: HEK.HAmIP cells, $\Delta[Ca^{2+}]_i$ = 112 ± 3.41 nM; HEK.mIP^{S357A} cells, $\Delta[Ca^{2+}]_i$ = 55.3 ± 2.57 nM.

kemia cells (13, 15, 38), and in human megakaryoblastic leukemia (MEG01) cells (39). Coupling of IP to changes in intracellular Ca^{2+}, rather than to activation of adenylyl cyclase, has been reported in rabbit cortical collecting ducts (40), whereas the IP expressed in the rat medullary thick ascending limb coupled exclusively to G_i-mediated inhibition of adenylyl cyclases rather than to G_s-mediated adenylyl cyclase activation (16). Whereas molecular cloning has confirmed the existence of single IPs in human, mouse, rat, and bovine tissues (11, 41–43), the cloned human and mouse IP are reported to couple to activation of both adenylyl cyclase and PLCβ effectors (10–13, 41). To date, IP isoforms are not known to exist unlike other prostanoid receptors, and thus it appears that differential mRNA splicing mechanisms *per se* cannot account for the multiple patterns of IP signaling within a given species (3, 44). Thus, the key objective of the present study was to investigate the molecular mechanisms whereby a single IP may couple to more than one G protein:effector system by examining in detail the signaling properties of the mIP either stably overexpressed in HEK 293 (HEK.mIP) cells or in native MEL cells.

Consistent with mIP coupling to Gα_s, stimulation of HEK.mIP and MEL cells resulted in significant cicaprost-induced increases in cAMP generation. However, contrary to previous reports, mIP expressed in both cell types also coupled to inhibition of adenylyl cyclase in a PTx-sensitive, Gα_i-dependent manner (data relating to PTx studies in MEL cells are not shown). The PKA inhibitor H-89 abolished mIP:Gα_i coupling in HEK.mIP cells but had no effect on mIP:Gα_s coupling. On the

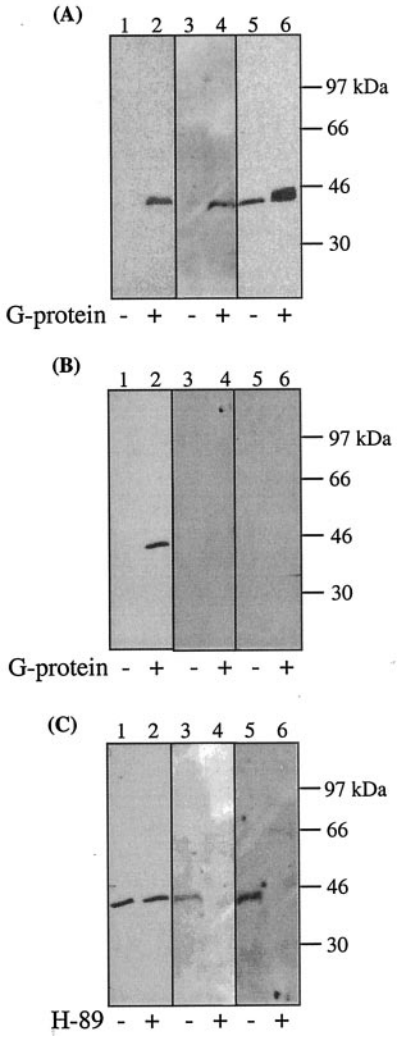

FIG. 11. **Co-immunoprecipitation of the mIP and mIP^{S357A} with their associated Gα subunits.** HEK.HAmIP isolate 2 (*panel A*) and HEK.HAmIP^{S357A} (*panel B*) cells were transiently co-transfected for 48 h without (−) or with (+) the cDNA encoding Gα_s (*panels A* and *B*, *lanes 1* and *2*), Gα_i (*panels A* and *B*, *lanes 3* and *4*), and Gα_q (*panels A* and B, *lanes 5* and *6*). Alternatively HEK.HAmIP isolate 2 cells (*panel C*) transiently co-transfected for 48 h with Gα_s (*panel C*, *lanes 1* and *2*), Gα_i (*panel C*, *lanes 3* and *4*), and Gα_q (*panel C*, *lanes 5* and *6*) were preincubated for 10 min with vehicle (−) or with 10 μM H-89 (+). Thereafter cells were stimulated with 1 μM cicaprost for 10 min, and HA epitope-tagged receptors were immunoprecipitated using the anti-HA antibody 101R. Immunoprecipitations were resolved by SDS-PAGE and electroblotted onto PVDF membranes. Membranes were screened for the presence of Gα_s (*panels A–C*, *lanes 1* and *2*), Gα_i (*Panels A–C*, *lanes 3* and *4*), or Gα_q (*panels A–C*, *lanes 5* and *6*) using the respective anti-Gα subunit antisera essentially as described under "Experimental Procedures," and immunoreactive bands were visualized by chemiluminescence detection. Data presented are representative of three independent experiments. The positions of the molecular mass markers (kDa) are indicated to the *right* of *panels A–C*.

other hand, the PKC inhibitor GF 109203X had no effect on mIP coupling to either Gα_s or Gα_i. To establish whether the specificity of mIP coupling to Gα_s or Gα_i was concentration-dependent, HEK.mIP cells were stimulated with a range of cicaprost concentrations in the absence and presence of forskolin. In the absence of forskolin, mIP generated significant, concentrationdependent increases in measurable cAMP consistent with its coupling to Gα_s. However, in the presence of forskolin, stimulation of mIP with low concentrations of cicaprost (<1 nM) generated significant concentration-dependent increases in measurable cAMP consistent with its coupling to Gα_s, whereas at higher concentrations (>1 nM) cicaprost yielded a concentrationdependent reduction in cAMP generation indicative of mIP coupling to Gα_i. Preincubation with PTx or H-89, but not GF 109203X (data not shown), blocked mIP-mediated Gα_i coupling but had no effect on mIP coupling to Gα_s over the range of cicaprost concentrations used. Taken together these data indicate that mIP can couple to both Gα_s and to PTx-sensitive Gα_i to mediate activation and inhibition of adenylyl cyclase, respectively. Coupling of mIP to Gα_i, but not Gα_s, appears to require a critical concentration of cAMP and is dependent on PKA activation.

We extended our studies to investigate the mechanism whereby the G_s-coupled mIP may also couple to PLC activation. Cicaprost stimulation of HEK.mIP cells led to significant increases in IP_3 generation and mobilization of $[Ca^{2+}]_i$. H-89, but not PTx or GF 109203X, almost completely abolished cicaprost-mediated signaling indicating that mIP-mediated IP_3 generation and $[Ca^{2+}]_i$ mobilization occurred in a PTx-insensitive, PKC-independent, PKA-dependent mechanism(s). Moreover, overexpression of the carboxyl-terminal residues of βARK1, to sequester G$\beta\gamma$ subunits, confirmed that cicaprost-mediated IP_3 generation (data not shown) or $[Ca^{2+}]_i$ mobilization were not through G$\beta\gamma$-stimulated mechanisms such as through G$\beta\gamma$ regulation of PLCβ isozymes (45). Consistent with these data, transient overexpression of Gα_q led to significant augmentations of cicaprost-mediated IP_3 generation and mobilization of $[Ca^{2+}]_i$ (Ref. 12 and data not shown) in a PTx-insensitive, PKC-independent, PKA-dependent mechanism(s). Furthermore, the PI-PLC inhibitor U73122 (32) abolished cicaprost-induced $[Ca^{2+}]_i$ mobilization confirming that the primary source of mIP-mediated $[Ca^{2+}]_i$ mobilization is from IP_3-regulated intracellular stores. Thus, taken together these data indicate that mIP, in addition to coupling to G_s and G_i, can couple to PLC and that PLC coupling occurs in a Gα_q-mediated, PTx-insensitive, PKC-independent, but PKA-dependent, manner. Additionally, coupling of mIP to both G_i and G_q is dependent on its prior coupling to G_s to stimulate cAMP-dependent PKA activation. Moreover, subsequent whole cell phosphorylation assays established that the mIP is subject to cicaprost-mediated phosphorylation in a GF 109203X-independent, H-89-dependent manner indicating that mIP coupling to Gα_i and Gα_q may involve direct PKA-mediated phosphorylation of the mIP itself.

We have previously established that mIP may be unique among GPCRs in that it is isoprenylated within its C-tail domain (12, 13). Disruption of isoprenylation through site-directed mutagenesis to generate mIP^{SSLC} established that isoprenylation of mIP is required for its efficient Gα_s- and Gα_q-mediated activation of adenylyl cyclase and PLC, respectively, suggesting that the C-tail of the mIP may be involved in receptor:G protein interaction (12). Consistent with previous studies (12), the isoprenylation-defective mIP^{SSLC} exhibited significantly diminished coupling to both adenylyl cyclase and PLC activation compared with the wild type mIP. Moreover, mIP^{SSLC} failed to couple to Gα_i to mediate inhibition of forskolin-induced cAMP generation indicating that (*a*) the C-tail domain of mIP may be involved in receptor:Gα_i interaction and/or that (*b*) failure of mIP^{SSLC} to couple to Gα_i may be due to its initial inability to couple to Gα_s to stimulate PKA-mediated mIP phosphorylation and subsequent coupling to Gα_i and indeed to Gα_q.

Analysis of the primary sequence of the mIP revealed the presence of a putative PKA phosphorylation site within the C-tail region of the mIP where Ser^{357} represents the predicted target residue for phosphorylation (34). Thus, through the use of site-directed mutagenesis, the role of Ser^{357} was investigated. Whereas mIP^{S357A} exhibited Gα_s activation of adenylyl

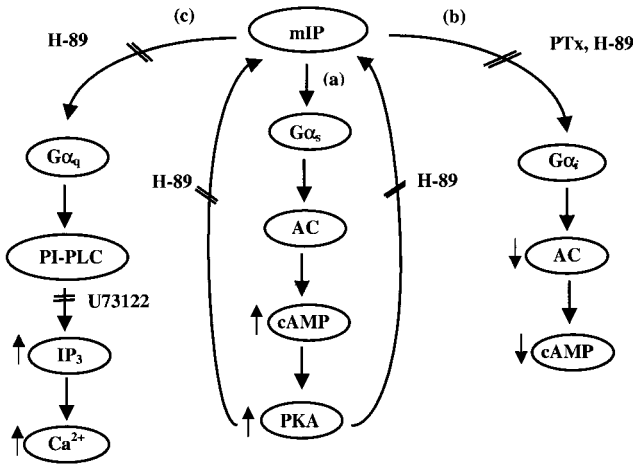

FIG. 12. **Model of mIP coupling to $G\alpha_s$-mediated activation of adenylyl cyclase (*AC*) (*a*), $G\alpha_i$-coupled inhibition of adenylyl cyclase (*b*), and $G\alpha_q$-coupled activation of PI-PLC (*c*).** *a*, ligand activation of the mIP stimulates $G\alpha_s$-mediated activation of adenylyl cyclase leading to increases in cAMP generation and, in turn, activation of PKA. *b*, activated PKA phosphorylates the mIP at Ser^{357} favoring mIP:$G\alpha_i$ coupling leading to decreases in adenylyl cyclase activity and, in turn, decreases in cAMP generation. PKA-mediated mIP phosphorylation and coupling to PTx-sensitive $G\alpha_i$ may be inhibited by H-89. *c*, alternatively PKA-mediated phosphorylation of mIP at Ser^{357} may promote mIP:$G\alpha_q$ coupling leading to activation of PI-PLC and, in turn, leading to increases in IP_3 generation and mobilization of $[Ca^{2+}]_i$. PKA-mediated mIP phosphorylation and coupling to $G\alpha_q$ may be inhibited by H-89, and the PI-PLC inhibitor U73122 blocks mIP-mediated IP_3 generation and mobilization of $[Ca^{2+}]_i$.

cyclase similar to that of the wild type mIP, it failed to couple to $G\alpha_i$ or to $G\alpha_q$ to mediate inhibition of adenylyl cyclase and activation of PLC, respectively. The fact that mIP, but not mIP^{S357A}, exhibited cicaprost-mediated $G\alpha_i$ and $G\alpha_q$ coupling confirmed that cicaprost is acting through the mIP itself and not through another, perhaps related prostanoid, receptor to mediate these effects. Unlike that which occurred for the wild type mIP, whole cell phosphorylation assays established that mIP^{S357A} did not undergo significant agonist-induced PKA phosphorylation. Finally, cicaprost stimulation of cells overexpressing HA epitope-tagged forms of the mIP and mIP^{S357A} permitted co-immunoprecipitation of $G\alpha_s$ confirming direct, agonist-induced interaction of both mIP and mIP^{S357A} with $G\alpha_s$. On the other hand, whereas stimulation of HEK.HAmIP cells with cicaprost resulted in co-precipitation of HAmIP with both $G\alpha_i$ and $G\alpha_q$, co-precipitation of neither $G\alpha_i$ nor $G\alpha_q$ along with $HAmIP^{S357A}$ was observed. Furthermore, in support of this, inhibition of PKA blocked co-precipitation of $G\alpha_i$ and $G\alpha_q$ with HAmIP but had no effect on co-precipitation of $G\alpha_s$ with HAmIP suggesting that for mIP interaction with $G\alpha_i$ and/or $G\alpha_q$ to occur mIP must be phosphorylated on Ser^{357} by PKA. Thus, taken together the data presented in this study provide a mechanism whereby the classical $G\alpha_s$-coupled mIP may couple both to $G\alpha_i$-mediated inhibition of adenylyl cyclase and to $G\alpha_q$-mediated activation of PLC. This mechanism, as outlined in the model presented in Fig. 12, requires initial mIP coupling to $G\alpha_s$ leading to elevation of cAMP and PKA activation. Thereafter PKA-mediated phosphorylation of mIP at Ser^{357} within the C-tail domain of mIP in turn favors its coupling to $G\alpha_i$, leading to inhibition of adenylyl cyclase, and to $G\alpha_q$, leading to activation of PLC.

The proposed mechanism of mIP coupling to both $G\alpha_s$ and to $G\alpha_i$ is not unlike that which has been previously reported for the β_2AR-mediated switching from $G\alpha_s$ to $G\alpha_i$ (21, 23). In their model, the β_2AR can switch coupling from $G\alpha_s$ to $G\alpha_i$ in a mechanism involving initial $G\alpha_s$ activation of adenylyl cyclase and subsequent PKA phosphorylation within the third intracellular loop of the β_2AR; the phosphorylated β_2AR, in turn, exhibited diminished coupling to $G\alpha_s$ and increased coupling to $G\alpha_i$ thereby switching its coupling from $G\alpha_s$ to $G\alpha_i$. (21, 23, 46). In our studies, we identified Ser^{357} within the C-tail of the mIP itself as being the critical residue for PKA phosphorylation and, hence, regulating the $G\alpha_s$ to $G\alpha_i$ coupling mechanism. Our studies do not rule out the possibility that other components of the signaling pathway may also be targets for the PKA-mediated phosphorylation and contribute to the differential signaling event; however, the fact that mIP^{S357A} can couple efficiently to G_s to generate cAMP and activate PKA but not to G_i makes it unlikely that other signaling elements are involved. One of the manifestations of the β_2AR switching its coupling from G_s is that the G_i-coupled receptor can stimulate activation of the mitogen-activated protein kinase cascades in a PTx-sensitive, $G\beta\gamma$- and Src-mediated cascade (23). Whether a similar mechanism applies to the G_i-coupled mIP will require further investigation.

Many G_s-coupled GPCRs can activate both cAMP and IP_3/Ca^{2+} signaling pathways, and three mechanisms have been proposed to explain this dual G protein coupling. One mechanism is independent GPCR coupling to G_s and to a G_q member, such as G_{15} or G_{16}, to initiate independent activation of adenylyl cyclase and PLCβ (24). The other two mechanisms involve cAMP-regulated PKA activation of PLCβ or PKA-induced switching of receptor coupling from G_s to G_i (24). In the latter mechanism, such as that reported to occur for the vasoactive intestinal peptide receptor, both PLC-mediated IP_3 generation and mobilization of $[Ca^{2+}]_i$ are regulated through PTx-sensitive, G_i-derived $G\beta\gamma$ subunits rather than through G_q-coupled mechanisms (24). In our studies investigating mIP, as stated, we established that PKA phosphorylation of Ser^{357} within the C-tail of the mIP itself as the critical residue to regulate coupling to both $G\alpha_i$ and $G\alpha_q$; thereafter the phosphorylated mIP can independently regulate G_i- and G_q-mediated inhibition of adenylyl cyclase and activation of PLC, respectively. Thus, our mechanism differs from that proposed for the vasoactive intestinal peptide receptor in that mIP-mediated PLC activation is PTx-insensitive, G_i- and $G\beta\gamma$-independent. Moreover, mIP-mediated PLC activation occurs in a PKA-dependent, G_q-coupled mechanism suggesting that mIP must undergo PKA-mediated switching from G_s to G_q to activate PLC activation as opposed to independently coupling to G_s and G_q members as proposed in the first mechanism (24). Similar to that previously stated for mIP:$G\alpha_i$ coupling, our studies do not fully exclude the possibility that other components of the signaling pathway, such as PLCβ, may also be targets for the PKA-mediated phosphorylation as proposed in the second mechanism (24); however, the fact that mIP^{S357A} can couple efficiently to G_s but does not couple to G_q:PLC activation makes it unlikely.

Several GPCRs are known to activate dual or multiple signaling systems, such as the thrombin receptor, the histamine H_2 receptor, or the parathyroid receptor to name but a few (47). In many instances, this can occur in a species- or cell type-specific manner. However, the molecular mechanisms whereby a given GPCR may couple to multiple G protein-coupled effectors are, on the whole, poorly understood. Our studies extend those previously reported for the β_2AR (23) and for the vasoactive peptide receptor (24) and establish that second messenger kinase-, such as PKA-mediated switching is not restricted to G_s/G_i mechanisms but may also be extended to dual switching from G_s to both G_i and G_q mechanisms independently. Moreover, our studies add further evidence to the growing awareness that mechanisms such as GPCR phosphorylation and internalization, previously thought to be exclusively asso-

ciated with the desensitization of GPCR signaling, may trigger activation of other signaling events, such as switching receptor coupling from one G protein-coupled cascade to other G protein-coupled cascade(s), or to initiation of other signaling events, such as activation of mitogen-activated protein kinase cascades and/or transactivation of growth factor signaling (21, 22).

REFERENCES

1. Campbell, W. B. (1990) in *Goodman and Gilman's The Pharmacological Basis of Therapeutics* (Gilman, A. G., Rall, T. W., Neis, A. S., and Taylor, P., eds) 8th Ed., pp. 600–617, Pergamon Press, New York
2. Vane, J. R., and Botting, R. M. (1995) *Am. J. Cardiol.* **75,** 3A–10A
3. Narumiya, S., Sugimoto, Y., and Fumitaka, U. (1999) *Physiol. Rev.* **79,** 1193–1226
4. Murata, T., Ushikubi, F., Matsuoka, T., Hirata, M., Yamasaki, A., Sugimoto, Y., Ichikawa, A., Aze, Y., Tanaka, T., Yoshida, N., Ueno, A., Oh-ishi, S., and Narumiya, S. (1997) *Nature* **388,** 678–682
5. Zucker, T. P., Bonisch, D., Hasse, A., Grosser, T., Weber, A. A., and Schrör, K. (1998) *Eur. J. Pharmacol.* **345,** 213–220
6. Sakai, A., Yajima, M., and Nishio, S. (1990) *Life Sci.* **47,** 711–719
7. Coleman, R. A., Smith, W. L., and Narumiya, S. (1994) *Pharmacol. Rev.* **46,** 205–229
8. Wise, H., and Jones, R. L. (1996) *Trends Pharmacol. Sci.* **17,** 17–21
9. Armstrong, R. A. (1996) *Pharmacol. Ther.* **72,** 171–191
10. Smyth, E. M., Li, W. H., and Fitzgerald, G. A. (1998) *J. Biol. Chem.* **273,** 23258–23266
11. Namba, T., Oida, H., Sugimoto, Y., Kakizuka, A., Negishi, M., Ichikawa, A., and Narumiya, S. (1994) *J. Biol. Chem.* **269,** 9986–9992
12. Hayes, J. S., Lawler, O. A., Walsh, M.-T., and Kinsella, B. T. (1999) *J. Biol. Chem.* **274,** 23707–23718
13. Lawler, O. A., Miggin, S. M., and Kinsella, B. T. (2001) *Br. J. Pharmacol.* **132,** 1639–1649
14. Siegel, G., Carl, A., Adler, A., and Stock, G. (1989) *Eicosanoids* **2,** 213–222
15. Schwaner, I., Offermanns, S., Spicher, K., Seifert, R., and Schultz, G. (1995) *Biochim. Biophys. Acta* **1265,** 8–14
16. Hebert, R. L., O'Connor, T., Neville, C., Burns, K. D., Laneuville, O., and Peterson, L. N. (1998) *Am. J. Physiol.* **275,** F904–F914
17. Leigh, P. J., and MacDermot, J. (1985) *Br. J. Pharmacol.* **85,** 237–247
18. Krane, A., MacDermot, J., and Keen, Ms. (1994) *Biochem. Pharmacol.* **47,** 953–959
19. Giovanazzi, S., Accomazzo, M. R., Letari, O., Oliva, D., and Nicosia, S. (1997) *Biochem. J.* **325,** 71–77
20. Smyth, E. M., Austin, S. C., Reilly, M. P., and Fitzgerald, G. A. (2000) *J. Biol. Chem.* **275,** 32037–32045
21. Lefkowitz, R. J. (1998) *J. Biol. Chem.* **273,** 18677–18680
22. Luttrell, L. M., Daaka, Y., and Lefkowitz, R. J. (1999) *Curr. Opin. Cell Biol.* **11,** 177–183
23. Daaka, Y., Luttrell., L. M., and Lefkowitz, R. J. (1997) *Nature* **390,** 88–91
24. Luo, X., Zeng, W., Xu, X., Popov, S., Davignon, I., Wilkie, T. M., Mumby, S. M., and Muallem, S. (1999) *J. Biol. Chem.* **274,** 17684–17690
25. Koch, W. J., Hawes, B. E., Inglese, J., Luttrell, L. M., and Lefkowitz, R. J. (1994) *J. Biol. Chem.* **269,** 6193–6197
26. Kinsella, B. T., O'Mahony, D. J., and Fitzgerald, G. A. (1997) *J. Pharmacol. Exp. Ther.* **281,** 957–964
27. Gagnon, A. W., Kallal, L., and Benovic, J. L. (1998) *J. Biol. Chem.* **273,** 6976–6981
28. Bradford, M. M. (1976) *Anal. Biochem.* **72,** 248–254
29. Walsh, M.-T., Foley, J. F., and Kinsella, B. T. (2000) *J. Biol. Chem.* **275,** 20412–20423
30. Godfrey, P. P. (1992) in *Signal Transduction: A Practical Approach* (Milligan, G., ed) pp. 105–120, IRL Press, Oxford
31. Thompson, A. K., Mostafapour, S. P., Denlinger, L. C., Bleasdale, J. E., and Fisher, S. K. (1991) *J. Biol. Chem.* **266,** 23856–23862
32. Kobayashi, H., Honma, S., Nakahata, N., and Ohizumi, Y. (2000) *J. Neurochem.* **74,** 2167–2173
33. Smyth, E. M., Nestor, P. V., and Fitzgerald, G. A. (1996) *J. Biol. Chem.* **271,** 33698–33704
34. Blom, N., Kreeqipuu, A., and Brunak, S. (1998) *Nucleic Acids Res.* **26,** 382–386
35. Dogne, J. M., de Leval, X., Delarge, J., David, J. L, Masereel, B. (2000) *Curr. Med. Chem.* **7,** 609–628
36. Oka, M., Negishi, M., Nishigaki, N., and Ichikawa, A. (1993) *Cell. Signal.* **5,** 643–650
37. Vassaux, G., Gaillard, D., Ailhaud, G., and Negrel, R. (1992) *J. Biol. Chem.* **267,** 11092–11097
38. Schwaner, I., Seifert, R., and Schultz, G. (1992) *Biochem. J.* **281,** 301–307
39. Watanabe, T., Yatomi, Y., Sunaga, S., Miki, I., Ishii, A., Nakao, A., Higashihara, M., Seyama, Y., Ogura, M., and Saito, H. (1991) *Blood* **78,** 2328–2336
40. Hebert, R. L., Regnier, L., and Peterson, L. N. (1995) *Am. J. Physiol.* **268,** F145–F154
41. Boie, Y., Rushmore, T. H., Darmon-Goodwin, A., Grygorczyk, R., Slipetz, D. M., Metters, K. M., and Abramovitz, M. (1994) *J. Biol. Chem.* **269,** 12173–12178
42. Nakagawa, O., Tanaka, I., Usui, T., Harada, M., Sasaki, Y., Itoh, H., Yoshimasa, T., Namba, T., Narumiya, S., and Nakao, K. (1994) *Circulation* **90,** 1643–1647
43. Sasaki, Y., Usui, T., Tanaka, I., Nakagawa, O., Sando, T., Takahashi, T., Namba, T., Narumiya, S., and Nakao, K. (1994) *Biochim. Biophys. Acta* **1224,** 601–605
44. Kilpatrick, G. J., Dautzenberg, F. M., Martin, G. R., and Eglen, R. M. (1999) *Trends Pharmacol. Sci.* **20,** 294–301
45. Singer, W. D., Brown, H. A., and Sternweis, P. C. (1997) *Annu. Rev. Biochem.* **66,** 475–509
46. Okamoto, T., Murayama, Y., Hayashi, Y., Inagaki, M., Ogata, E., and Nishimoto, I. (1991) *Cell* **67,** 723–730
47. Watson, S., and Arkinstall, S. (eds) (1994) *The G-protein Linked Receptor Factsbook*, Academic Press, London

Protein Kinase A-mediated Phosphorylation of Serine 357 of the Mouse Prostacyclin Receptor Regulates Its Coupling to G_s-, to G_i-, and to G_q-coupled Effector Signaling

Orlaith A. Lawler, Sinead M. Miggin and B. Therese Kinsella

J. Biol. Chem. 2001, 276:33596-33607.
doi: 10.1074/jbc.M104434200 originally published online July 6, 2001

VOLUME 276 (2001) PAGES 33596–33607
DOI 10.1074/jbc.AAC118.004491

Protein kinase A-mediated phosphorylation of serine 357 of the mouse prostacyclin receptor regulates its coupling to G_s-, to G_i-, and to G_q-coupled effector signaling.

Orlaith A. Lawler, Sinead M. Miggin, and B. Therese Kinsella

PAGE 33605:

During a recent review of this article, the authors realized that there may have been unspecified reordering of lanes in Fig. 11*B* and possible duplication of *lanes 2* between Fig. 11, *B* and *C*. As the original data were no longer available, replicate data are provided. This correction does not affect the results or conclusions of this work. The authors wish to apologize for any inconvenience this error may have caused.

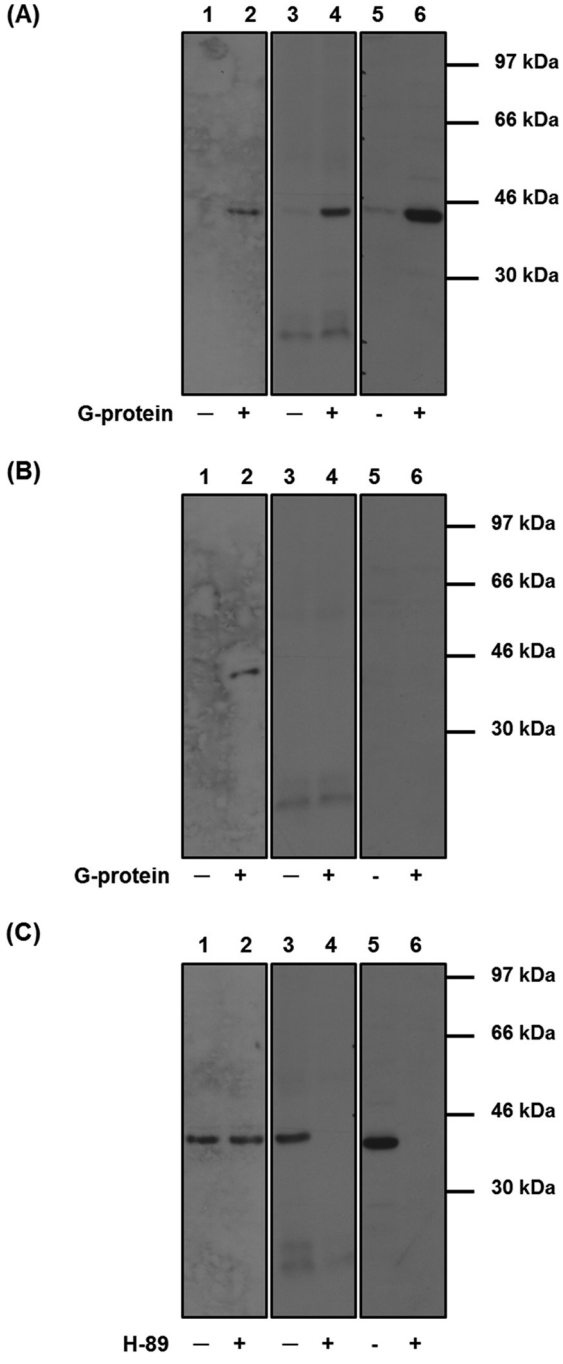

Fig. 11